

Progress Towards a Hybrid Renormalized Gluon PDF



MICHIGAN STATE
UNIVERSITY

William Good^{1*}
Kinza Hasan¹, Huey-Wen Lin¹
08.14.2024

LaMET2024 - University of Maryland

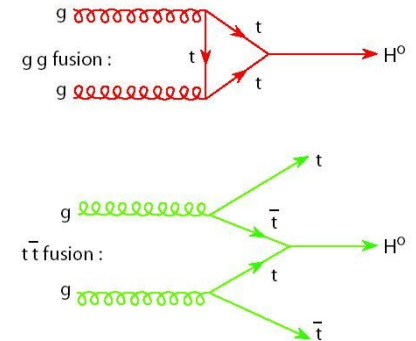
¹University of Michigan Department of Physics and Astronomy

*Speaker: goodwil9@msu.edu



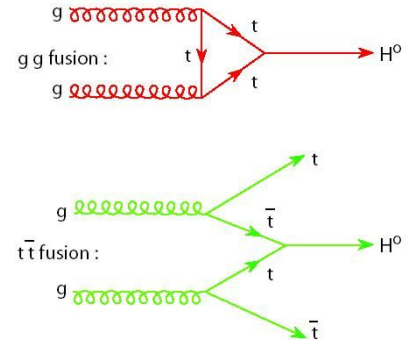
Introduction

- The gluon parton distribution function (PDF) provides important input to high energy experiments, such as Higgs production and J/ψ photo-production



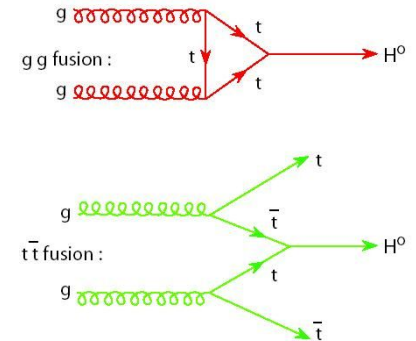
Introduction

- The gluon parton distribution function (PDF) provides important input to high energy experiments, such as Higgs production and J/ψ photo-production
- Phenomenological (pheno.) studies of the gluon PDF have some difficulties in obtaining the PDF in the “large”- x region, where lattice methods works better



Introduction

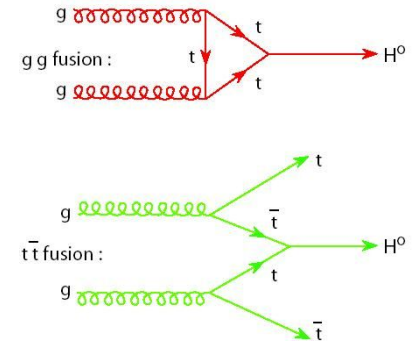
- The gluon parton distribution function (PDF) provides important input to high energy experiments, such as Higgs production and J/ψ photo-production
- Phenomenological (pheno.) studies of the gluon PDF have some difficulties in obtaining the PDF in the “large”- x region, where lattice methods works better
 - This is still difficult because there is some freedom of choice in the operators for the gluon PDF and these operators only have noisy, disconnected diagram contributions



Introduction

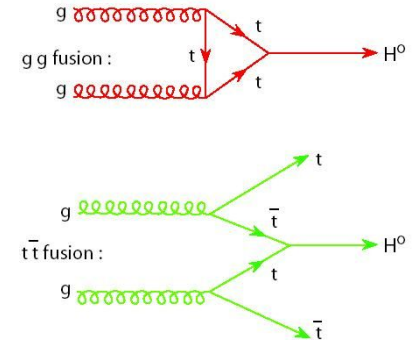
- The gluon parton distribution function (PDF) provides important input to high energy experiments, such as Higgs production and J/ψ photo-production
- Phenomenological (pheno.) studies of the gluon PDF have some difficulties in obtaining the PDF in the “large”- x region, where lattice methods works better
 - This is still difficult because there is some freedom of choice in the operators for the gluon PDF and these operators only have noisy, disconnected diagram contributions
- All previous lattice studies of the gluon PDF have used the pseudo-PDF methodology, which relies on fitting to a model of the PDF

Radyushkin PRD 96:034025 (2017)



Introduction

- The gluon parton distribution function (PDF) provides important input to high energy experiments, such as Higgs production and J/ψ photo-production
- Phenomenological (pheno.) studies of the gluon PDF have some difficulties in obtaining the PDF in the “large”- x region, where lattice methods works better
 - This is still difficult because there is some freedom of choice in the operators for the gluon PDF and these operators only have noisy, disconnected diagram contributions
- All previous lattice studies of the gluon PDF have used the pseudo-PDF methodology, which relies on fitting to a model of the PDF
Radyushkin PRD 96:034025 (2017)
- We present an explorative study of unpolarized gluon PDF operators from the LaMET framework



Operator and Matrix Elements

- The relevant operators for the gluon PDF are typically of this form or combinations of this form

$$O^{\mu\nu}(z) = F_a^{\mu\gamma}(z)W(z,0)F_{a,\gamma}^\nu(0)$$

Operator and Matrix Elements

- The relevant operators for the gluon PDF are typically of this form or combinations of this form

$$O^{\mu\nu}(z) = F_a^{\mu\gamma}(z)W(z,0)F_{a,\gamma}^\nu(0)$$

- $W(z,0)$ is a straight Wilson line in the z -direction with length z :

$$W(z,0) = \mathcal{P} \exp \left[-ig \int_0^z dz' A^z(z') \right]$$

Operator and Matrix Elements

- The relevant operators for the gluon PDF are typically of this form or combinations of this form

$$O^{\mu\nu}(z) = F_a^{\mu\gamma}(z)W(z,0)F_{a,\gamma}^\nu(0)$$

- $W(z,0)$ is a straight Wilson line in the z -direction with length z :

$$W(z,0) = \mathcal{P} \exp \left[-ig \int_0^z dz' A^z(z') \right]$$

- Only some choices of summation scheme for γ and combinations of these forms are multiplicatively renormalizable (MR)

Operator and Matrix Elements

- The relevant operators for the gluon PDF are typically of this form or combinations of this form

$$O^{\mu\nu}(z) = F_a^{\mu\gamma}(z)W(z,0)F_{a,\gamma}^\nu(0)$$

- $W(z,0)$ is a straight Wilson line in the z -direction with length z :

$$W(z,0) = \mathcal{P} \exp \left[-ig \int_0^z dz' A^z(z') \right]$$

- Only some choices of summation scheme for γ and combinations of these forms are multiplicatively renormalizable (MR)
- The relevant matrix elements for a hadron H are

$$h^B(z, P_z) = \langle H(P_z) | O(z) | H(P_z) \rangle$$

Some Historical Overview

- 2018: our group made some guesses on what operators could work and compared to the Fourier transform of a pheno. PDF **Fan, et al., PRL 121:242001 (2018)**
- 2019: several operators were shown to be MR and qPDF matching kernels were derived. One of the operators with the cleanest signal from the 2018 study was shown to be not MR **Zhang, et al., PRL 121:142001 (2019)**
Wang, et al. PRD 100:074509 (2019)
- 2020: A new operator was identified which was MR, but only the pseudo-PDF matching kernels were given explicitly **Balitsky, et al., PLB 808:135621 (2020)**
- Onwards: the new operator became very popular and was used to get PDFs through the pseudo-PDF method in several studies

Fan, et al. Int. J. Mod. Phys. A 36:12:2150080 (2021)
Khan, et al. (HadStruc) PRD 104:094516 (2021)
Fan, et al. PLB 823:136778 (2021)
Salas-Chavira, et al. PRD 106:094510 (2022)
Fan, WG, Lin. PRD 108:014508 (2023)
Delmar, et al. PRD 108:094515 (2023)

Operators of Focus

Zhang, et al., PRL 121:142001 (2019)

Wang, et al. PRD 100:074509 (2019)

Yao, et al. JHEP 11(2023)021

- A paper came out last year detailing hybrid renormalization matching for two of the previously identified operators:
 - Summation for i, j over transverse indices only. Summation for μ over all Lorentz indices

$$O^{(1)}(z) = F^{zi}(z)W(z, 0)F_i^z(0) \quad O^{(2)}(z) = F^{z\mu}(z)W(z, 0)F_\mu^z(0)$$

Operators of Focus

Zhang, et al., PRL 121:142001 (2019)

Wang, et al. PRD 100:074509 (2019)

Yao, et al. JHEP 11(2023)021

- A paper came out last year detailing hybrid renormalization matching for two of the previously identified operators:

- Summation for i, j over transverse indices only. Summation for μ over all Lorentz indices

$$O^{(1)}(z) = F^{zi}(z)W(z, 0)F_i^z(0) \quad O^{(2)}(z) = F^{z\mu}(z)W(z, 0)F_\mu^z(0)$$

- We want to see if we can achieve reasonable signal for these operators and compare them to what has been identified as a clean, seemingly less contaminated operator used in pseudo-PDF studies:

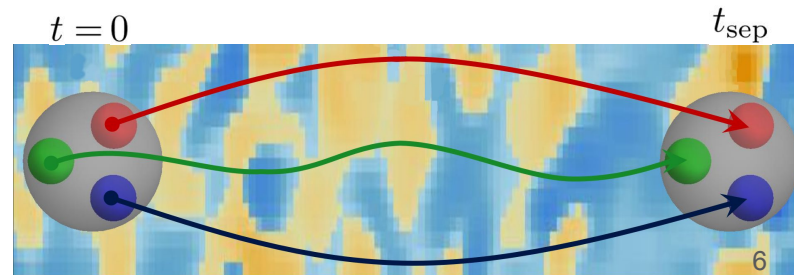
Balitsky, et al., PLB 808:135621 (2020)

$$O^{(3)}(z) = F^{ti}(z)W(z, 0)F_i^t(0) - F^{ij}(z)W(z, 0)F_{ij}(0)$$

Lattice Information

Follana *et al.* PRD 75:054502, 2007.
Bazavov, *et al.* [MILC], PRD 82:074501 2010.
Bazavov, *et al.* [MILC], PRD 87:054505 2013.
Bazavov, *et al.* [F Lattice and MILC] PRD 98:074512
2018

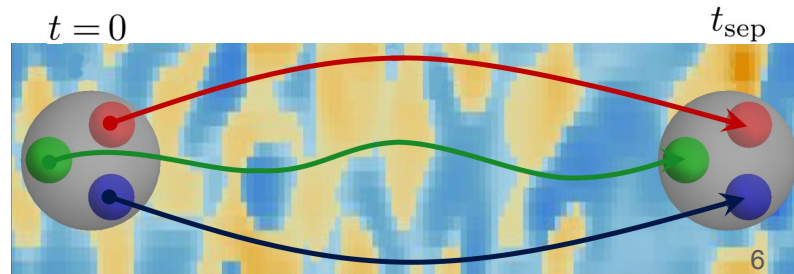
- Used lattices with $N_f = 2 + 1 + 1$ highly improved staggered quarks generated by the MILC collaboration with Wilson-clover fermions used in the valence sector



Lattice Information

Follana *et al.* PRD 75:054502, 2007.
Bazavov, *et al.* [MILC], PRD 82:074501 2010.
Bazavov, *et al.* [MILC], PRD 87:054505 2013.
Bazavov, *et al.* [F Lattice and MILC] PRD 98:074512
2018

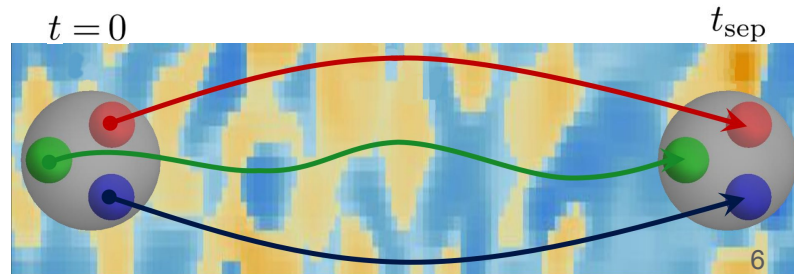
- Used lattices with $N_f = 2 + 1 + 1$ highly improved staggered quarks generated by the MILC collaboration with Wilson-clover fermions used in the valence sector
- We use lattice spacing $a \approx 0.12$ fm, and tune valence pion masses to $M_\pi \approx 310$ and 690 MeV with volume $24^3 \times 64$



Lattice Information

Follana *et al.* PRD 75:054502, 2007.
Bazavov, *et al.* [MILC], PRD 82:074501 2010.
Bazavov, *et al.* [MILC], PRD 87:054505 2013.
Bazavov, *et al.* [F Lattice and MILC] PRD 98:074512
2018

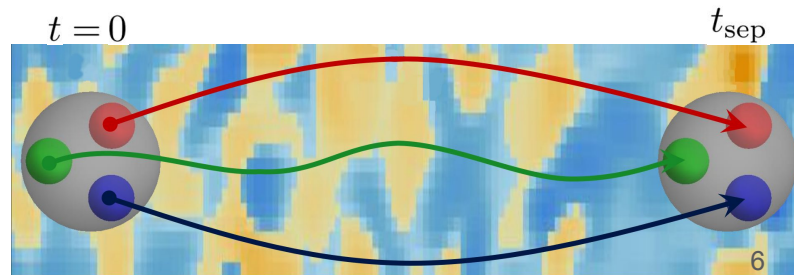
- Used lattices with $N_f = 2 + 1 + 1$ highly improved staggered quarks generated by the MILC collaboration with Wilson-clover fermions used in the valence sector
- We use lattice spacing $a \approx 0.12$ fm, and tune valence pion masses to $M_\pi \approx 310$ and 690 MeV with volume $24^3 \times 64$
- ~ 1.2 M 2-point (2pt) correlator measurements over 1013 configurations



Lattice Information

Follana *et al.* PRD 75:054502, 2007.
Bazavov, *et al.* [MILC], PRD 82:074501 2010.
Bazavov, *et al.* [MILC], PRD 87:054505 2013.
Bazavov, *et al.* [F Lattice and MILC] PRD 98:074512
2018

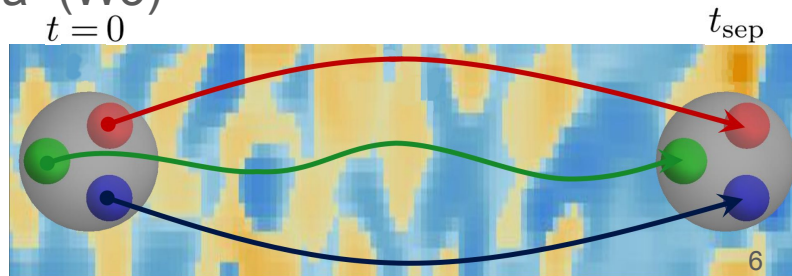
- Used lattices with $N_f = 2 + 1 + 1$ highly improved staggered quarks generated by the MILC collaboration with Wilson-clover fermions used in the valence sector
- We use lattice spacing $a \approx 0.12$ fm, and tune valence pion masses to $M_\pi \approx 310$ and 690 MeV with volume $24^3 \times 64$
- ~ 1.2 M 2-point (2pt) correlator measurements over 1013 configurations
- Gaussian momentum smearing to get signal up to 2.14 GeV boost momentum



Lattice Information

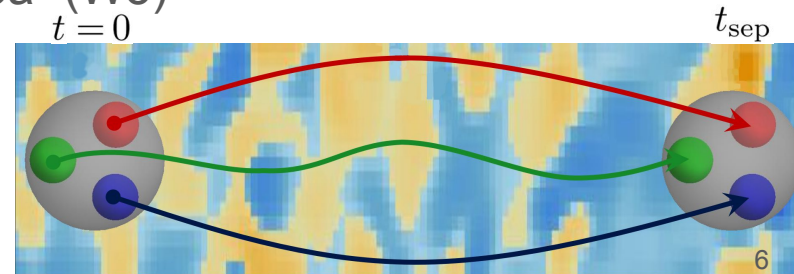
Follana *et al.* PRD 75:054502, 2007.
Bazavov, *et al.* [MILC], PRD 82:074501 2010.
Bazavov, *et al.* [MILC], PRD 87:054505 2013.
Bazavov, *et al.* [F Lattice and MILC] PRD 98:074512
2018

- Used lattices with $N_f = 2 + 1 + 1$ highly improved staggered quarks generated by the MILC collaboration with Wilson-clover fermions used in the valence sector
- We use lattice spacing $a \approx 0.12$ fm, and tune valence pion masses to $M_\pi \approx 310$ and 690 MeV with volume $24^3 \times 64$
- ~ 1.2 M 2-point (2pt) correlator measurements over 1013 configurations
- Gaussian momentum smearing to get signal up to 2.14 GeV boost momentum
- Two gauge link smearing sets for the 3-point (3pt) correlators: 5 steps of hypercubic smearing (HYP5) and Wilson flow with time $t=3a^2$ (W3)



Lattice Information

- Used lattices with $N_f = 2 + 1 + 1$ highly improved staggered quarks generated by the MILC collaboration with Wilson-clover fermions used in the valence sector
- We use lattice spacing $a \approx 0.12$ fm, and tune valence pion masses to $M_\pi \approx 310$ and 690 MeV with volume $24^3 \times 64$
- ~ 1.2 M 2-point (2pt) correlator measurements over 1013 configurations
- Gaussian momentum smearing to get signal up to 2.14 GeV boost momentum
- Two gauge link smearing sets for the 3-point (3pt) correlators: 5 steps of hypercubic smearing (HYP5) and Wilson flow with time $t=3a^2$ (W3)
- We look at the “strange” nucleon (N_s), light nucleon (N_l), strange pion (η_s), and the light pion (π)



LaMET Methodology

Ji, PRL 110:262002 (2013).

Ji, Sci. China Phys. Mech. Astron. 57:1407 (2014).

(Nice review: Ji, *et. al.* PRM 93:035005 (2021))

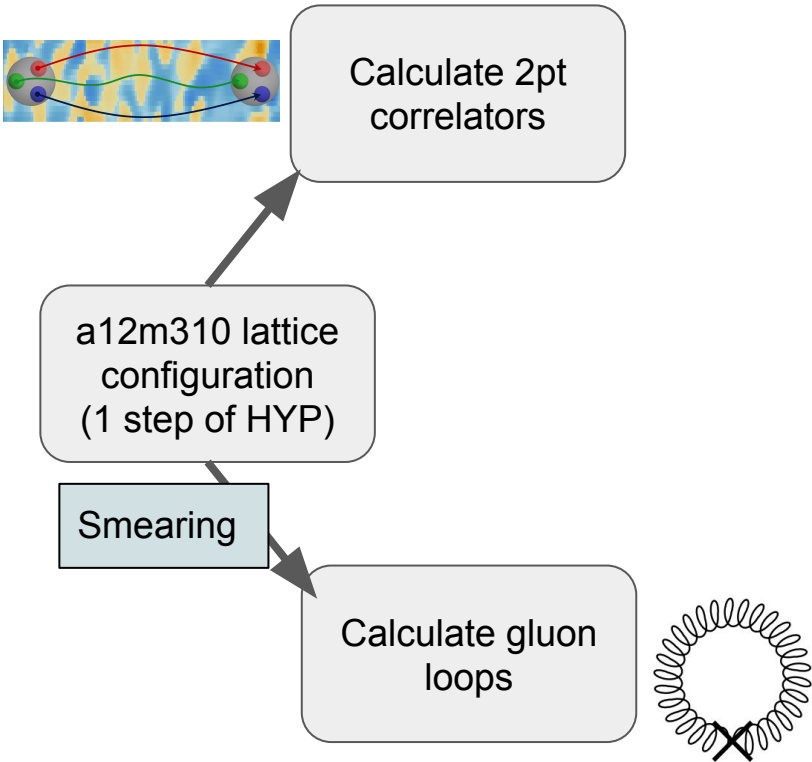
a12m310 lattice
configuration
(1 step of HYP)

LaMET Methodology

Ji, PRL 110:262002 (2013).

Ji, Sci. China Phys. Mech. Astron. 57:1407 (2014).

(Nice review: Ji, *et. al.* PRM 93:035005 (2021))

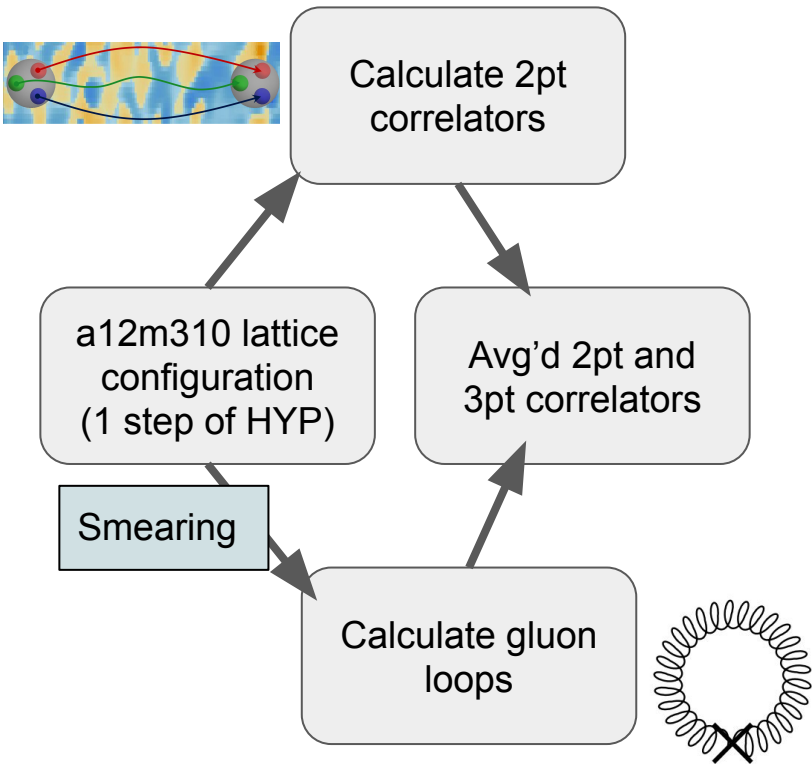


LaMET Methodology

Ji, PRL 110:262002 (2013).

Ji, Sci. China Phys. Mech. Astron. 57:1407 (2014).

(Nice review: Ji, *et. al.* PRM 93:035005 (2021))

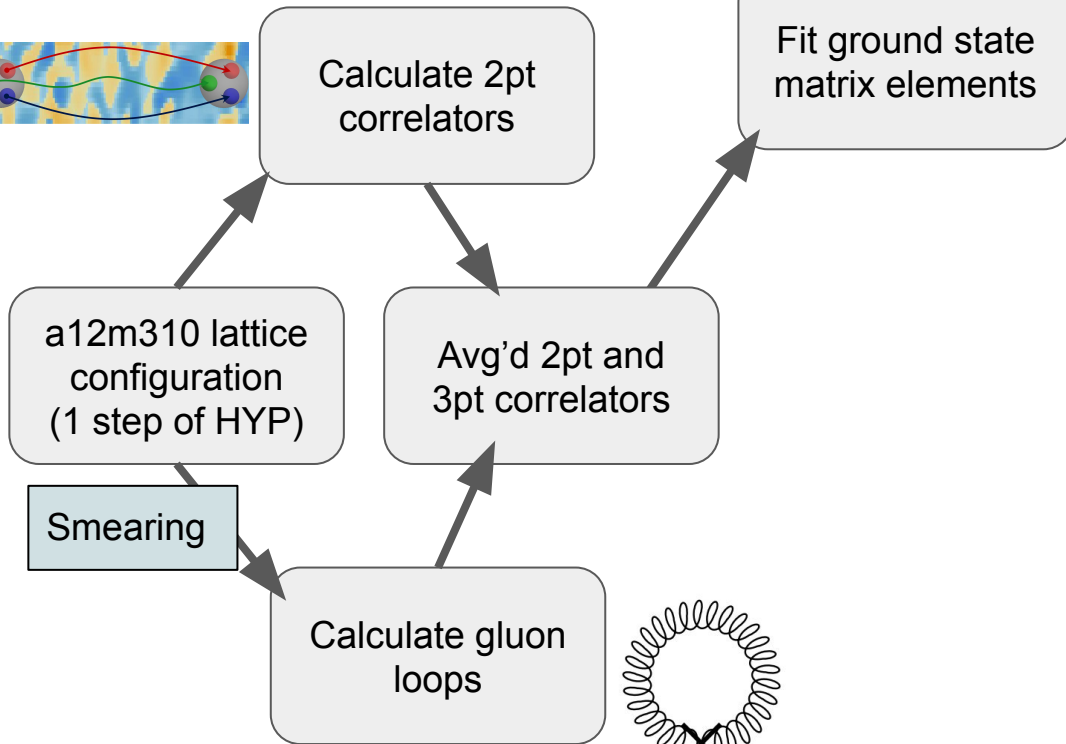
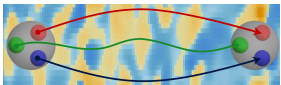


LaMET Methodology

Ji, PRL 110:262002 (2013).

Ji, Sci. China Phys. Mech. Astron. 57:1407 (2014).

(Nice review: Ji, *et. al.* PRM 93:035005 (2021))



$$h^B(z, P_z)$$

Fit ground state matrix elements

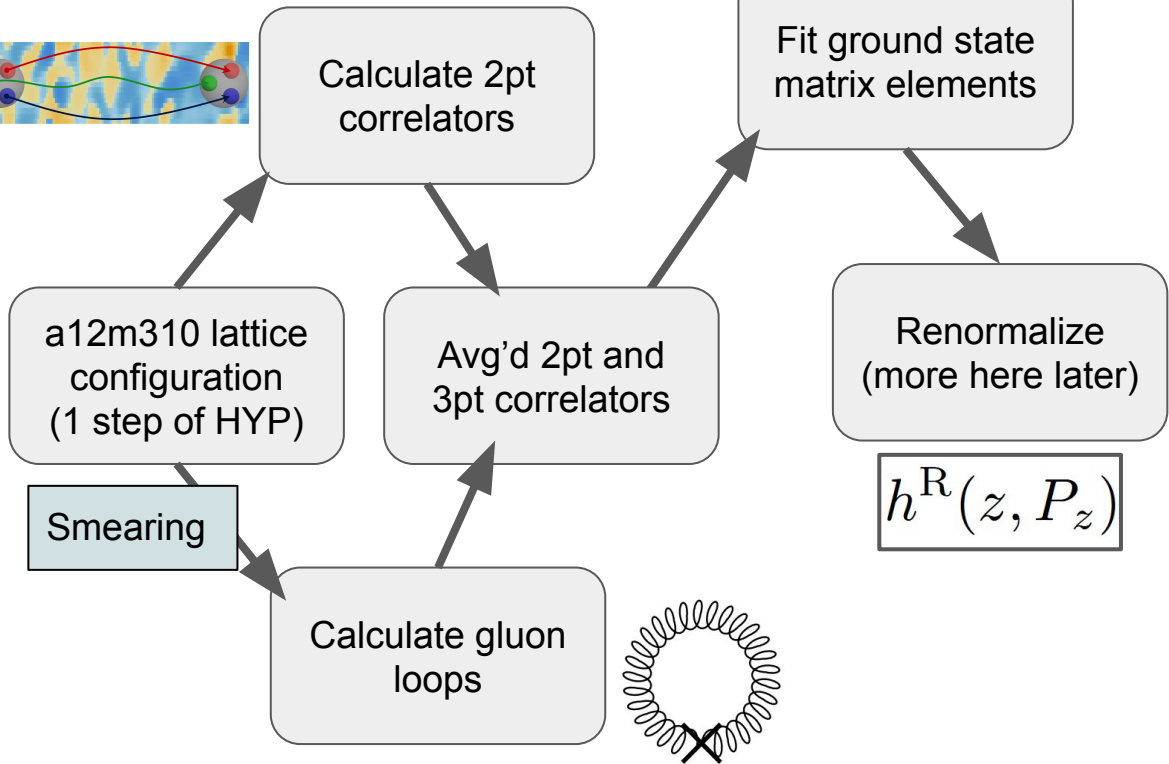
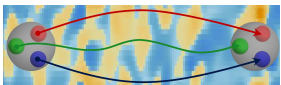
Smearing

Calculate gluon loops



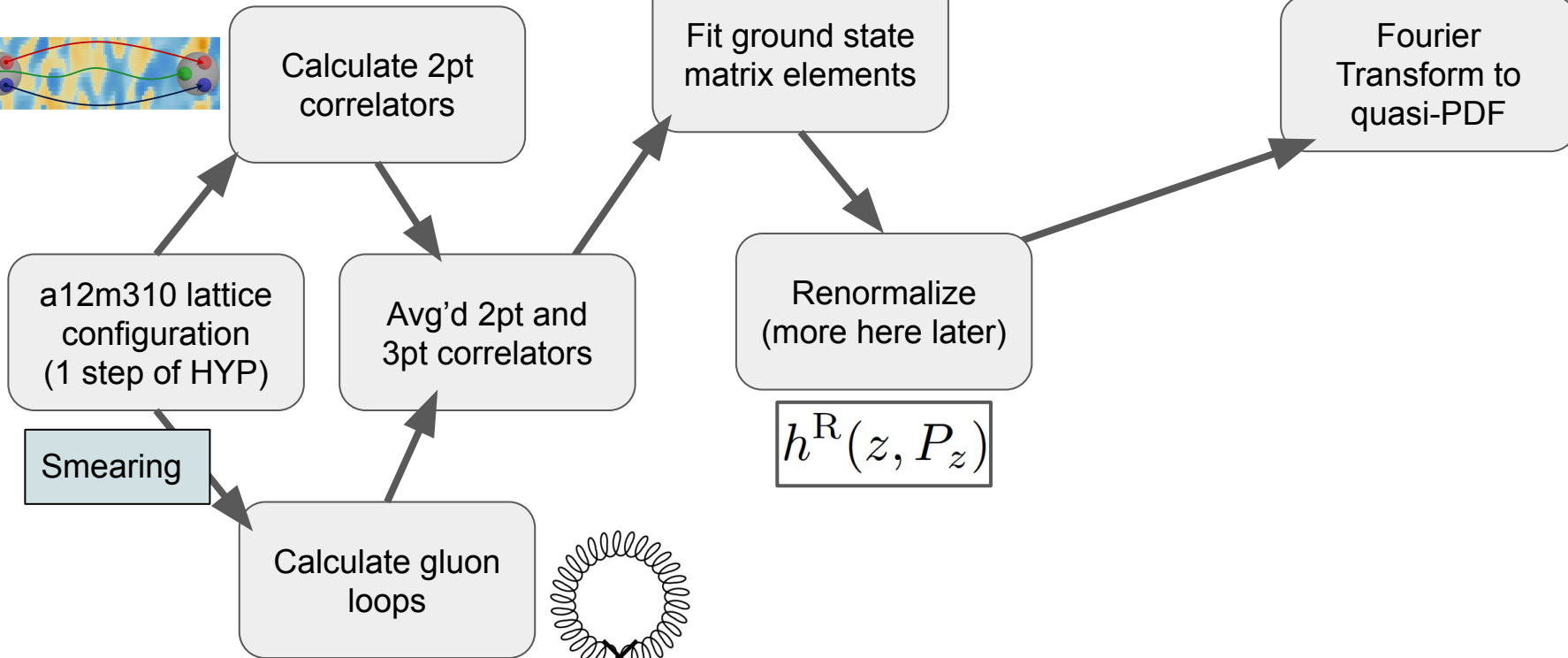
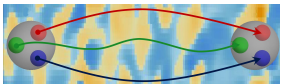
LaMET Methodology

Ji, PRL 110:262002 (2013).
Ji, Sci. China Phys. Mech. Astron. 57:1407 (2014).
(Nice review: Ji, *et. al.* PRM 93:035005 (2021))



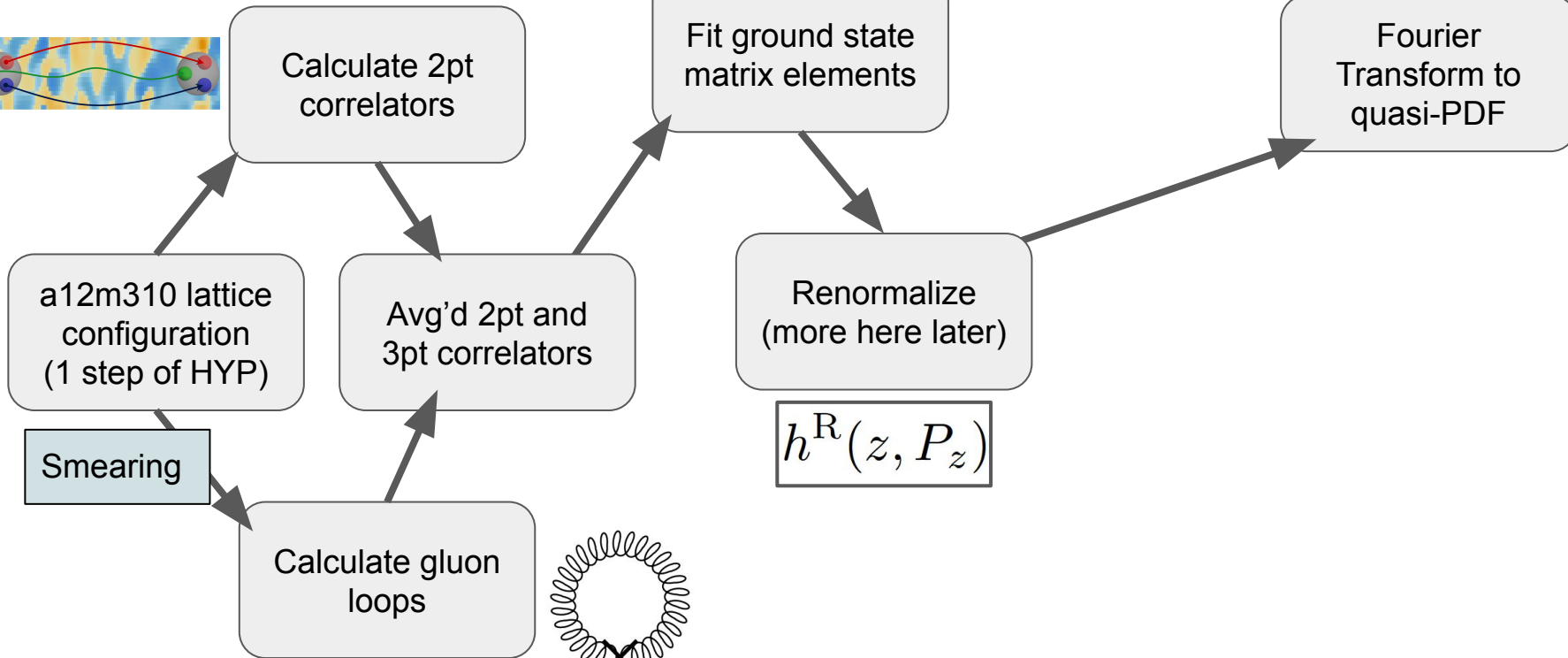
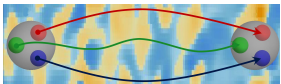
LaMET Methodology

Ji, PRL 110:262002 (2013).
Ji, Sci. China Phys. Mech. Astron. 57:1407 (2014).
(Nice review: Ji, *et. al.* PRM 93:035005 (2021))



LaMET Methodology

Ji, PRL 110:262002 (2013).
Ji, Sci. China Phys. Mech. Astron. 57:1407 (2014).
(Nice review: Ji, et. al. PRM 93:035005 (2021))

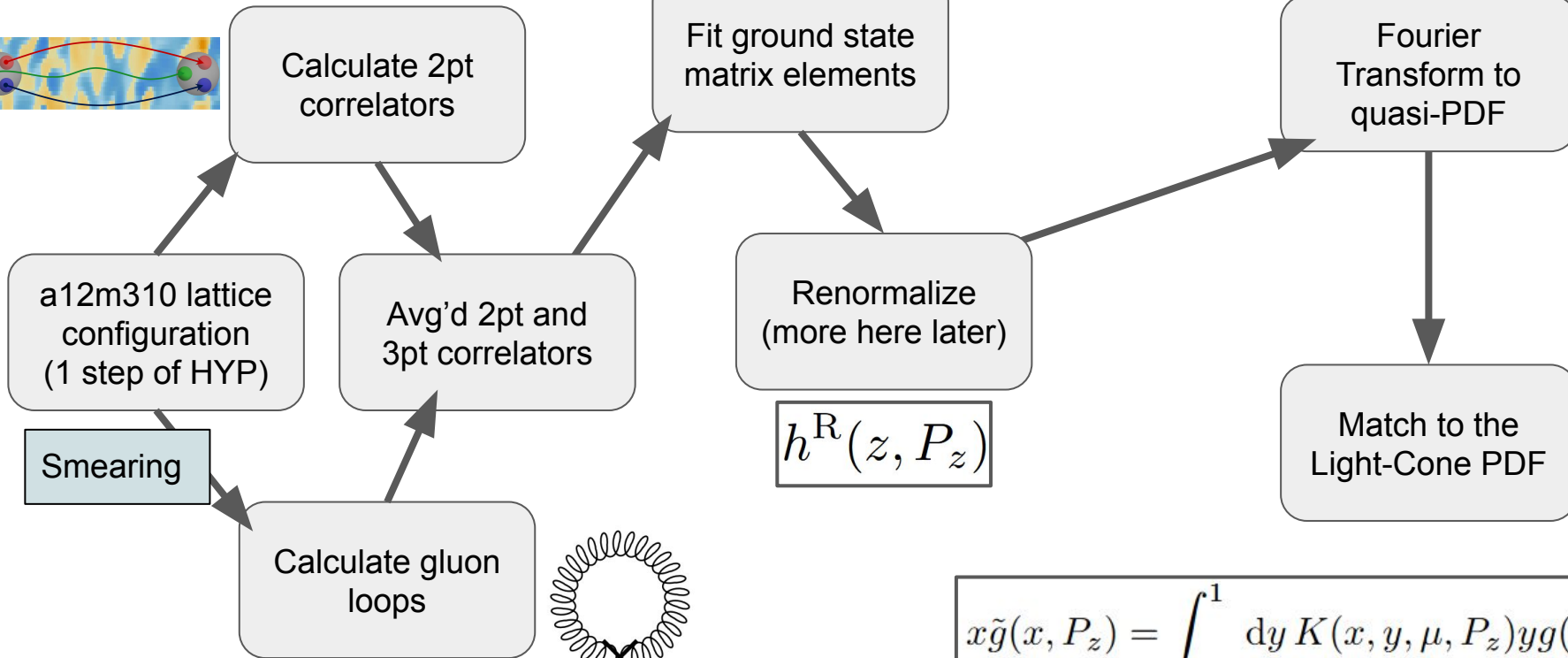
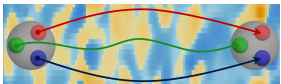


$$x\tilde{g}(x, P_z) = \int_{-\infty}^{\infty} \frac{dz}{2\pi P_z} e^{ixP_z z} h^R(z, P_z)$$



LaMET Methodology

Ji, PRL 110:262002 (2013).
 Ji, Sci. China Phys. Mech. Astron. 57:1407 (2014).
 (Nice review: Ji, *et. al.* PRM 93:035005 (2021))



$$x\tilde{g}(x, P_z) = \int_{-\infty}^{\infty} \frac{dz}{2\pi P_z} e^{ixP_z z} h^R(z, P_z)$$

$$x\tilde{g}(x, P_z) = \int_{-1}^1 dy K(x, y, \mu, P_z) yg(y, \mu)$$

2pt and 3pt Analysis

- Can fit the correlators to a two-state simultaneous fit:

$$C_H^{2\text{pt}}(P_z, t) = |A_{H,0}|^2 e^{-E_{H,0}t} + |A_{H,1}|^2 e^{-E_{H,1}t} + \dots$$

2pt and 3pt Analysis

- Can fit the correlators to a two-state simultaneous fit:

$$C_H^{2\text{pt}}(P_z, t) = |A_{H,0}|^2 e^{-E_{H,0}t} + |A_{H,1}|^2 e^{-E_{H,1}t} + \dots$$

$$C_H^{3\text{pt}}(z, P_z, t, t_{\text{sep}}) = |A_{H,0}|^2 \langle 0|O^{(i)}|0\rangle e^{-E_{H,0}t_{\text{sep}}} + |A_{H,0}||A_{H,1}| \langle 0|O^{(i)}|1\rangle e^{-E_{H,1}(t_{\text{sep}}-t)} e^{-E_{H,0}t} \\ + |A_{H,0}||A_{H,1}| \langle 1|O^{(i)}|0\rangle e^{-E_{H,0}(t_{\text{sep}}-t)} e^{-E_{H,1}t} + |A_{H,1}|^2 \langle 1|O^{(i)}|1\rangle e^{-E_{H,1}t_{\text{sep}}} + \dots$$

2pt and 3pt Analysis

- Can fit the correlators to a two-state simultaneous fit:

$$C_H^{2\text{pt}}(P_z, t) = |A_{H,0}|^2 e^{-E_{H,0}t} + |A_{H,1}|^2 e^{-E_{H,1}t} + \dots$$

$$C_H^{3\text{pt}}(z, P_z, t, t_{\text{sep}}) = |A_{H,0}|^2 \langle 0|O^{(i)}|0\rangle e^{-E_{H,0}t_{\text{sep}}} + |A_{H,0}||A_{H,1}| \langle 0|O^{(i)}|1\rangle e^{-E_{H,1}(t_{\text{sep}}-t)} e^{-E_{H,0}t}$$

$$+ |A_{H,0}||A_{H,1}| \langle 1|O^{(i)}|0\rangle e^{-E_{H,0}(t_{\text{sep}}-t)} e^{-E_{H,1}t} + |A_{H,1}|^2 \langle 1|O^{(i)}|1\rangle e^{-E_{H,1}t_{\text{sep}}} + \dots$$

2pt and 3pt Analysis

- Can fit the correlators to a two-state simultaneous fit:

$$C_H^{2\text{pt}}(P_z, t) = |A_{H,0}|^2 e^{-E_{H,0}t} + |A_{H,1}|^2 e^{-E_{H,1}t} + \dots$$

$$C_H^{3\text{pt}}(z, P_z, t, t_{\text{sep}}) = |A_{H,0}|^2 \langle 0|O^{(i)}|0\rangle e^{-E_{H,0}t_{\text{sep}}} + |A_{H,0}||A_{H,1}| \langle 0|O^{(i)}|1\rangle e^{-E_{H,1}(t_{\text{sep}}-t)} e^{-E_{H,0}t} \\ + |A_{H,0}||A_{H,1}| \langle 1|O^{(i)}|0\rangle e^{-E_{H,0}(t_{\text{sep}}-t)} e^{-E_{H,1}t} + |A_{H,1}|^2 \langle 1|O^{(i)}|1\rangle e^{-E_{H,1}t_{\text{sep}}} + \dots$$

- We can plot the ratio of the 3pt to 2pt which goes to $\langle 0|O^{(i)}|0\rangle$ at large separation times

$$R_H(P_z; t_{\text{sep}}, t) = \frac{C_H^{3\text{pt}}(P_z; t_{\text{sep}}, t)}{C_H^{2\text{pt}}(P_z; t_{\text{sep}})}$$

2pt and 3pt Analysis

- Can fit the correlators to a two-state simultaneous fit:

$$C_H^{2\text{pt}}(P_z, t) = |A_{H,0}|^2 e^{-E_{H,0}t} + |A_{H,1}|^2 e^{-E_{H,1}t} + \dots$$

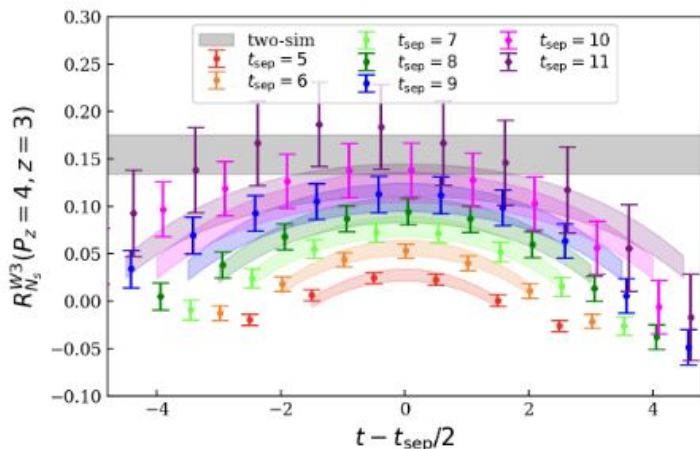
$$C_H^{3\text{pt}}(z, P_z, t, t_{\text{sep}}) = |A_{H,0}|^2 \langle 0|O^{(i)}|0\rangle e^{-E_{H,0}t_{\text{sep}}} + |A_{H,0}||A_{H,1}| \langle 0|O^{(i)}|1\rangle e^{-E_{H,1}(t_{\text{sep}}-t)} e^{-E_{H,0}t} \\ + |A_{H,0}||A_{H,1}| \langle 1|O^{(i)}|0\rangle e^{-E_{H,0}(t_{\text{sep}}-t)} e^{-E_{H,1}t} + |A_{H,1}|^2 \langle 1|O^{(i)}|1\rangle e^{-E_{H,1}t_{\text{sep}}} + \dots$$

- We can plot the ratio of the 3pt to 2pt which goes to $\langle 0|O^{(i)}|0\rangle$ at large separation times

N_s W3

$$R_H(P_z; t_{\text{sep}}, t) = \frac{C_H^{3\text{pt}}(P_z; t_{\text{sep}}, t)}{C_H^{2\text{pt}}(P_z; t_{\text{sep}})}$$

$O^{(2)}(z)$



Thanks to
Kinza
Hasan for
these plots

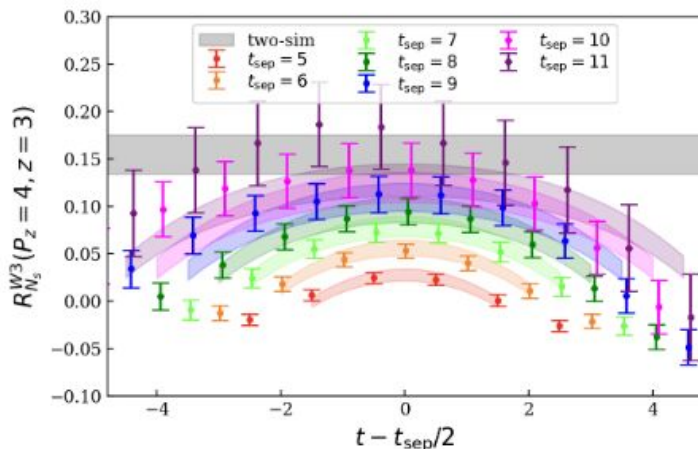
2pt and 3pt Analysis

- Can fit the correlators to a two-state simultaneous fit:

$$C_H^{2\text{pt}}(P_z, t) = |A_{H,0}|^2 e^{-E_{H,0}t} + |A_{H,1}|^2 e^{-E_{H,1}t} + \dots$$

$$C_H^{3\text{pt}}(z, P_z, t, t_{\text{sep}}) = |A_{H,0}|^2 \langle 0|O^{(i)}|0\rangle e^{-E_{H,0}t_{\text{sep}}} + |A_{H,0}||A_{H,1}| \langle 0|O^{(i)}|1\rangle e^{-E_{H,1}(t_{\text{sep}}-t)} e^{-E_{H,0}t} \\ + |A_{H,0}||A_{H,1}| \langle 1|O^{(i)}|0\rangle e^{-E_{H,0}(t_{\text{sep}}-t)} e^{-E_{H,1}t} + |A_{H,1}|^2 \langle 1|O^{(i)}|1\rangle e^{-E_{H,1}t_{\text{sep}}} + \dots$$

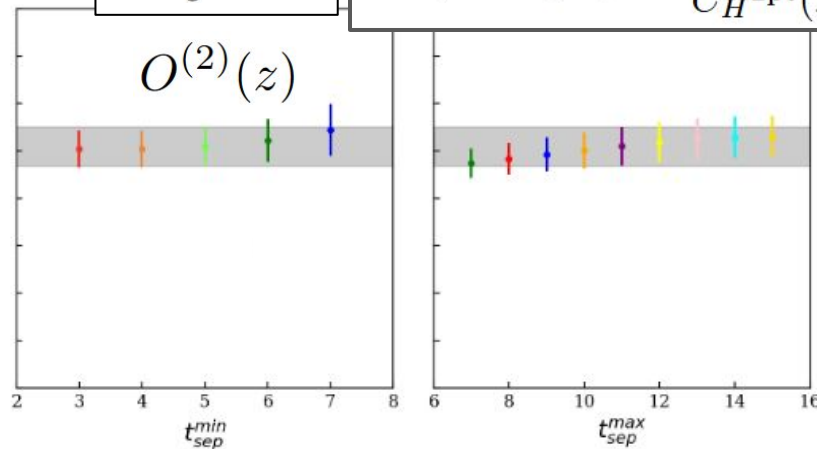
- We can plot the ratio of the 3pt to 2pt which goes to $\langle 0|O^{(i)}|0\rangle$ at large separation times



N_s W3

$O^{(2)}(z)$

$$R_H(P_z; t_{\text{sep}}, t) = \frac{C_H^{3\text{pt}}(P_z; t_{\text{sep}}, t)}{C_H^{2\text{pt}}(P_z; t_{\text{sep}})}$$



Thanks to Kinza Hasan for these plots

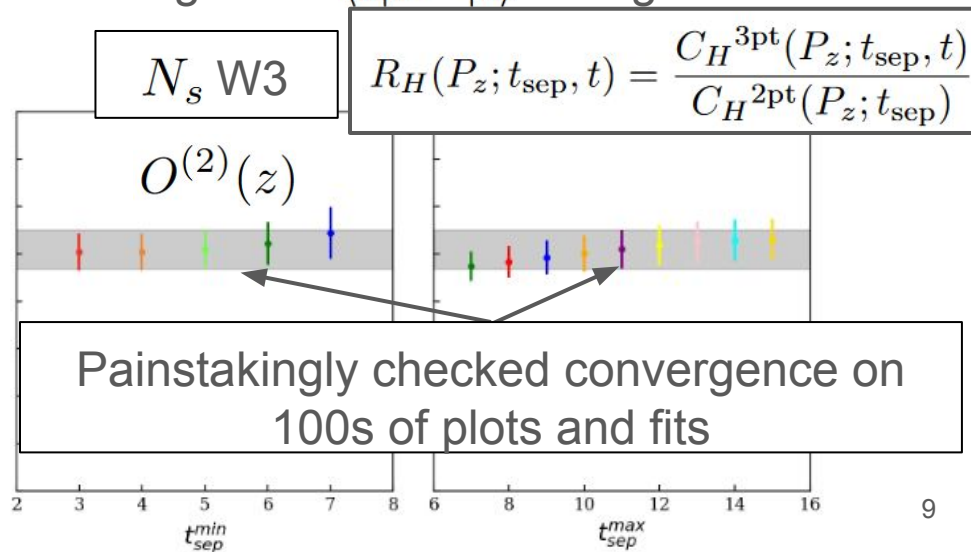
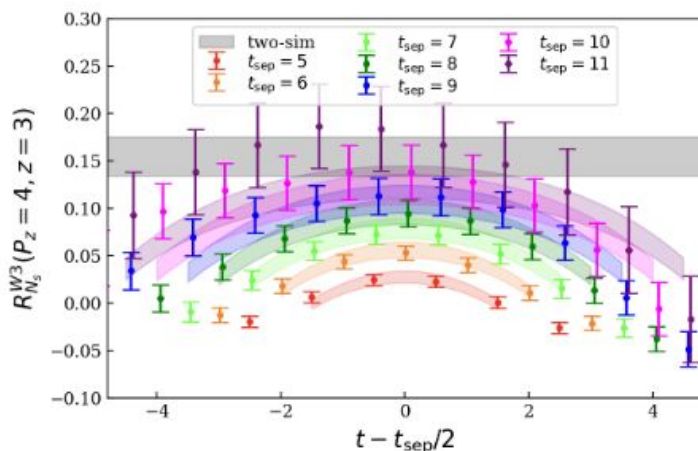
2pt and 3pt Analysis

- Can fit the correlators to a two-state simultaneous fit:

$$C_H^{2\text{pt}}(P_z, t) = |A_{H,0}|^2 e^{-E_{H,0}t} + |A_{H,1}|^2 e^{-E_{H,1}t} + \dots$$

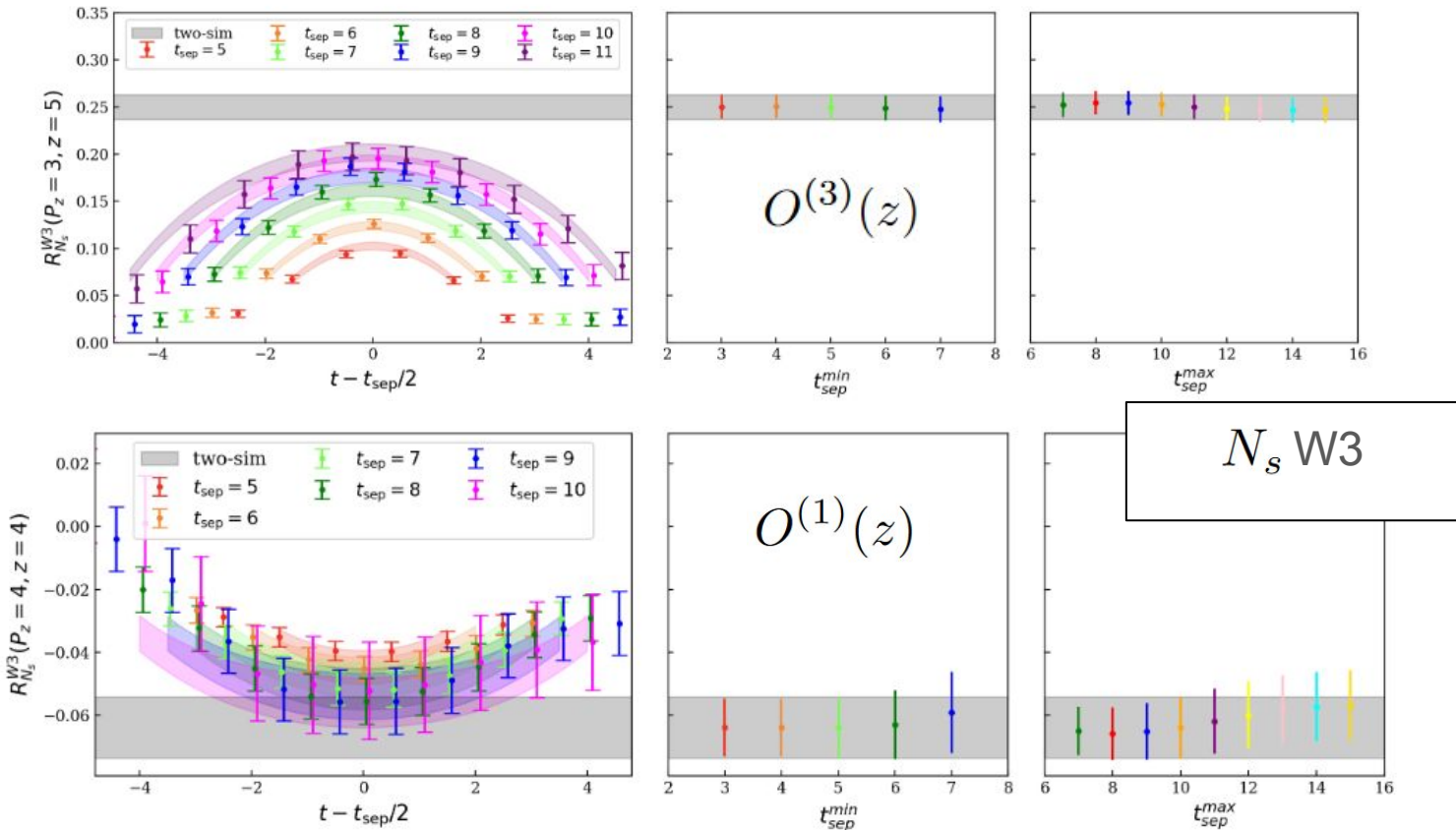
$$C_H^{3\text{pt}}(z, P_z, t, t_{\text{sep}}) = |A_{H,0}|^2 \langle 0|O^{(i)}|0\rangle e^{-E_{H,0}t_{\text{sep}}} + |A_{H,0}||A_{H,1}| \langle 0|O^{(i)}|1\rangle e^{-E_{H,1}(t_{\text{sep}}-t)} e^{-E_{H,0}t} \\ + |A_{H,0}||A_{H,1}| \langle 1|O^{(i)}|0\rangle e^{-E_{H,0}(t_{\text{sep}}-t)} e^{-E_{H,1}t} + |A_{H,1}|^2 \langle 1|O^{(i)}|1\rangle e^{-E_{H,1}t_{\text{sep}}} + \dots$$

- We can plot the ratio of the 3pt to 2pt which goes to $\langle 0|O^{(i)}|0\rangle$ at large separation times



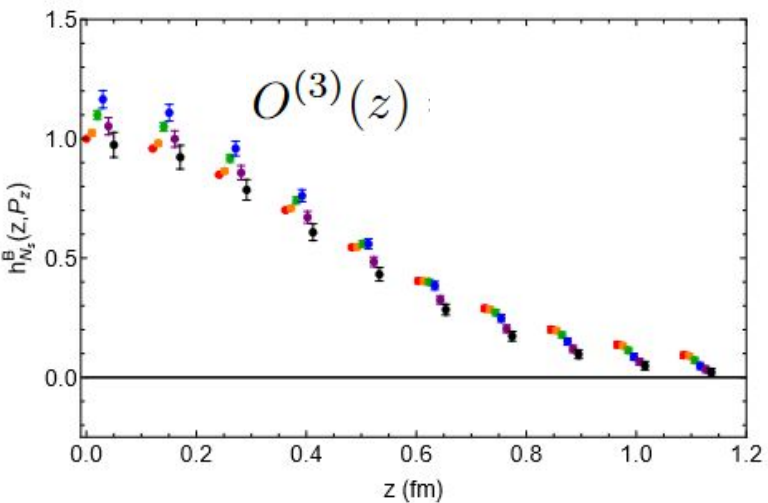
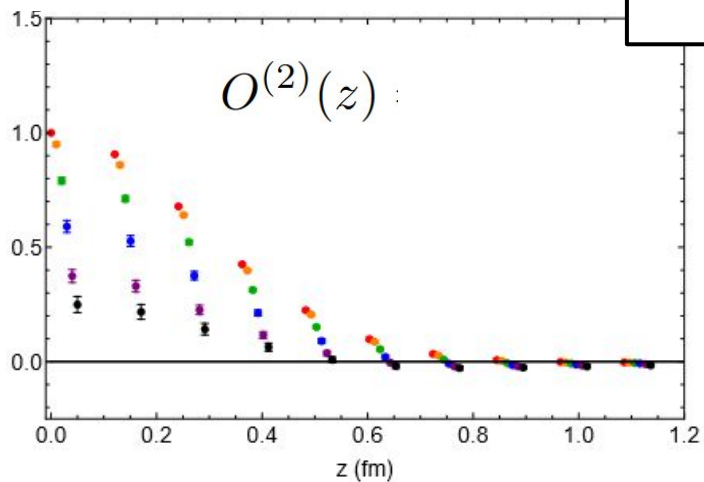
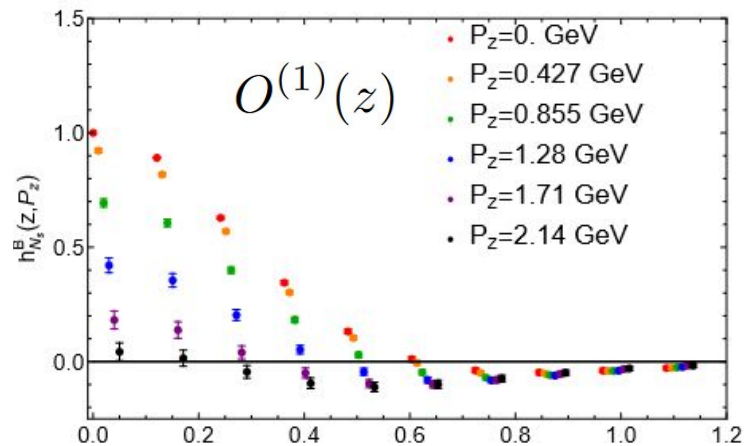
Thanks to Kinza Hasan for these plots

More Ratio Plots



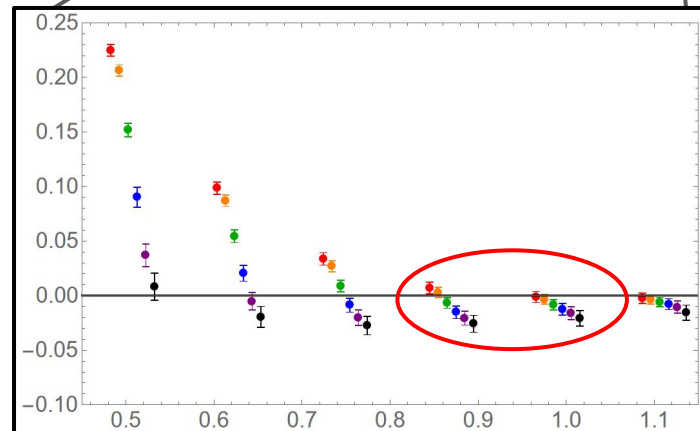
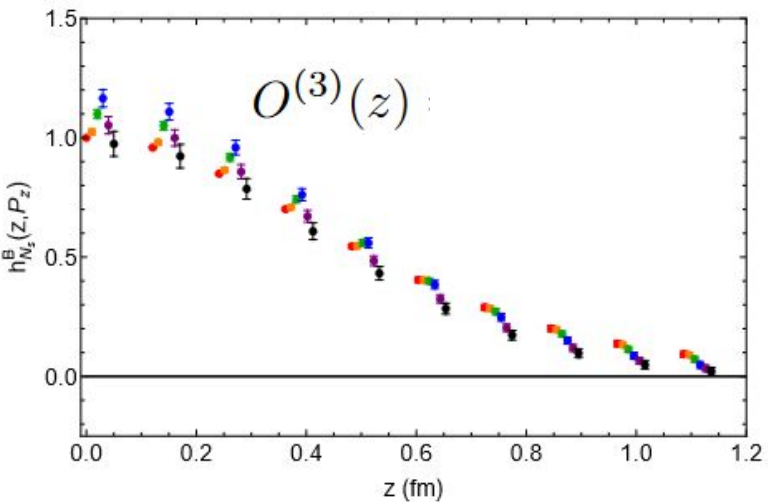
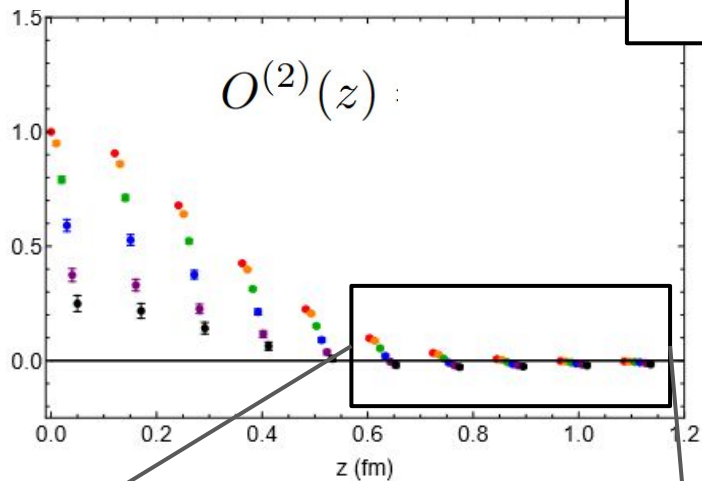
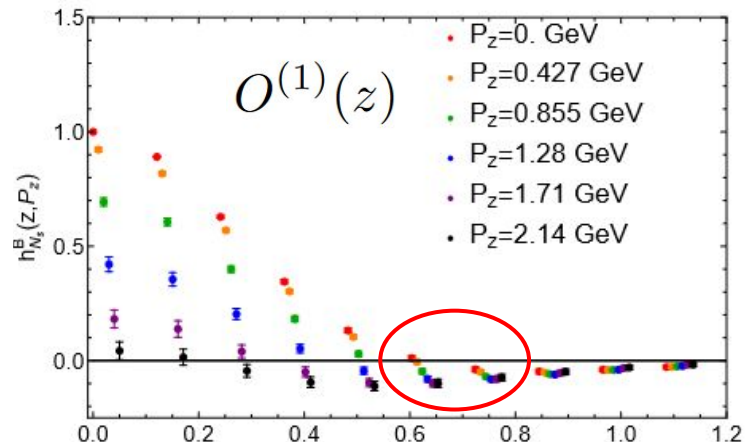
Bare Matrix Element Plots

N_s W3



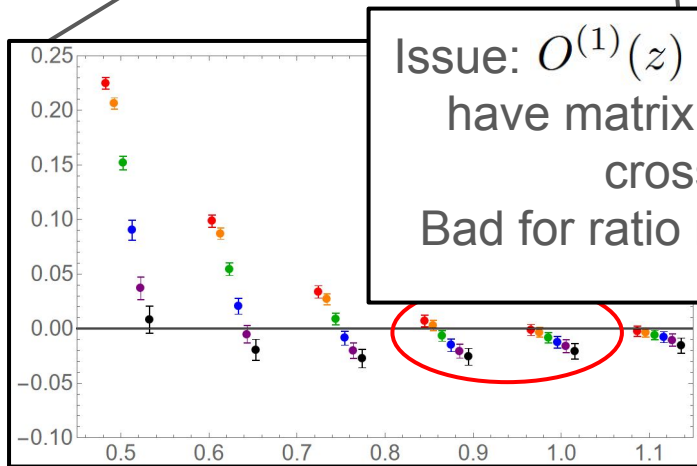
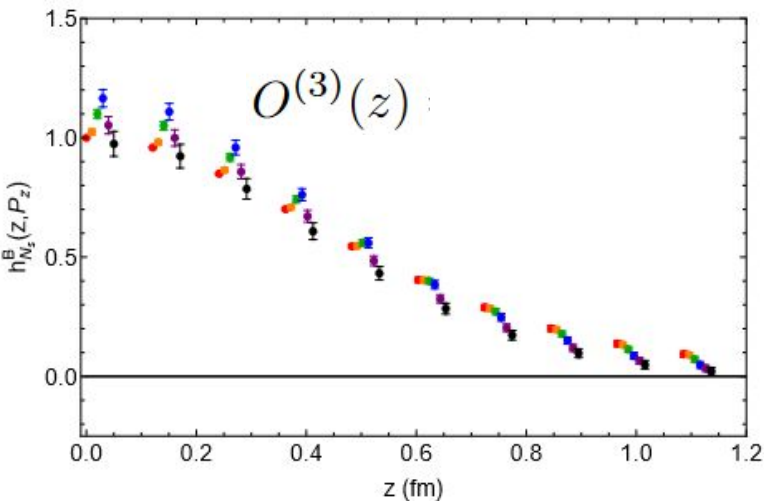
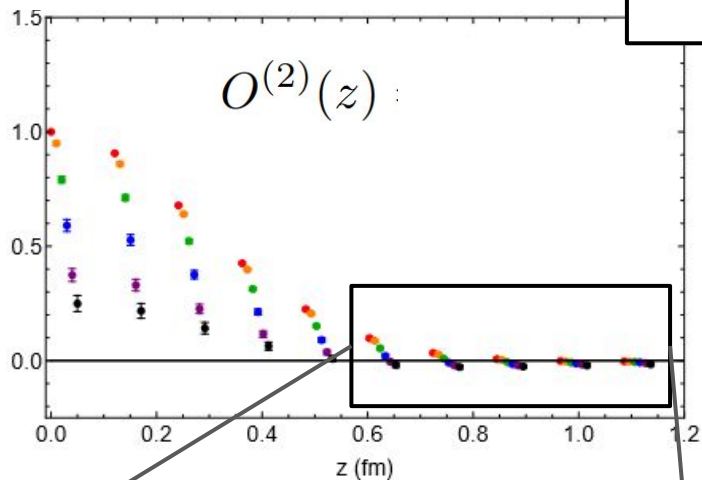
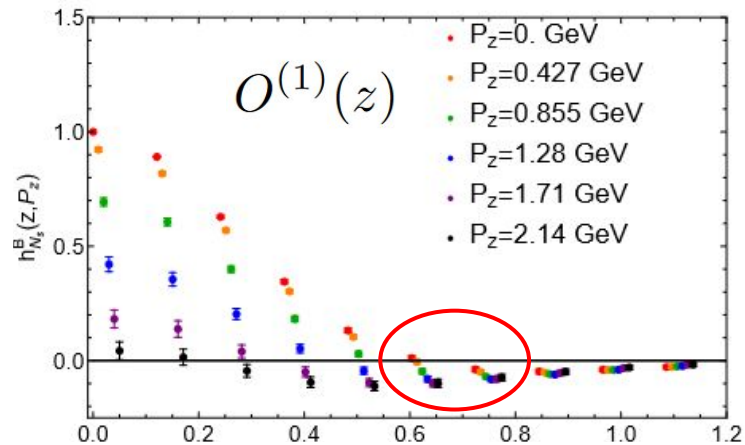
Bare Matrix Element Plots

N_s W3



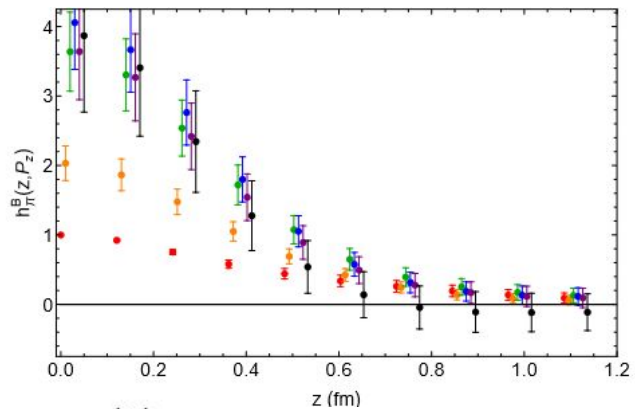
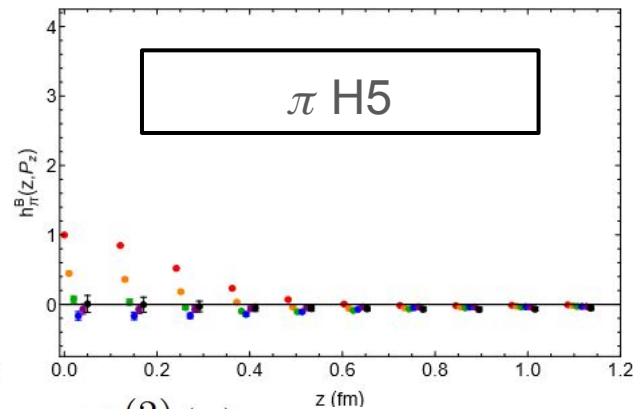
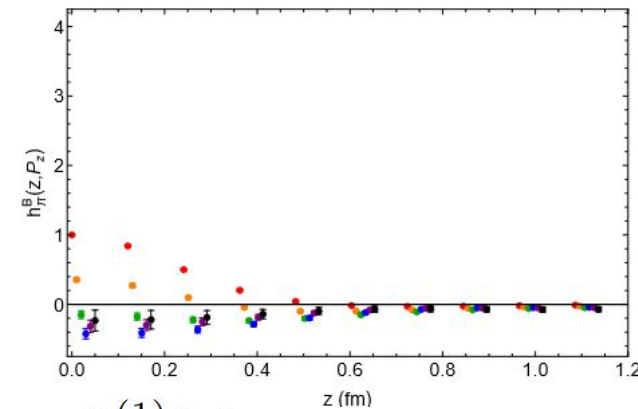
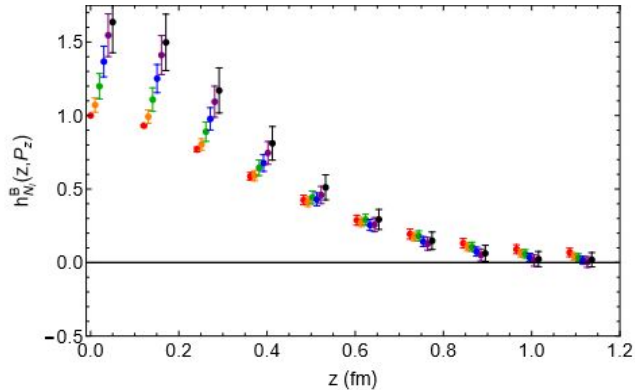
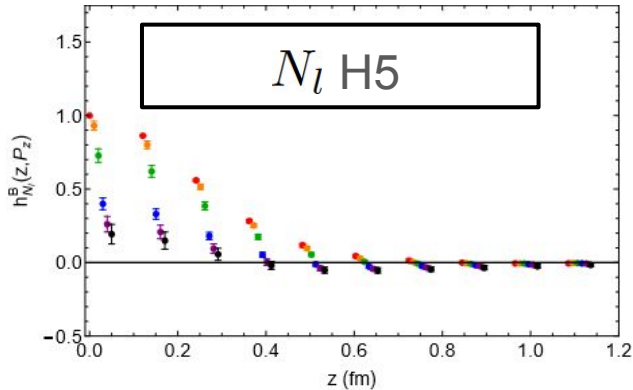
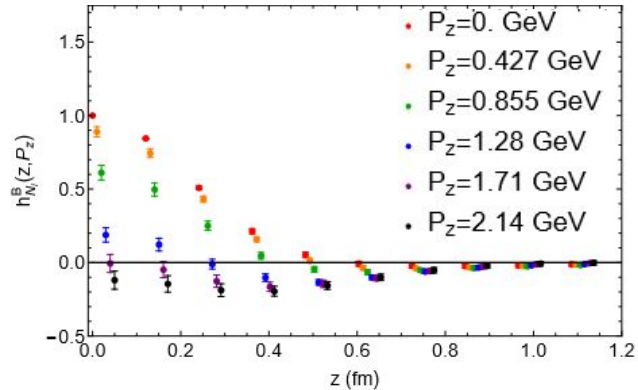
Bare Matrix Element Plots

N_s W3



Issue: $O^{(1)}(z)$ and $O^{(2)}(z)$ both have matrix elements that cross zero.
Bad for ratio renormalization

Similar Issues in Other Hadrons and Smearing Choice



$O^{(1)}(z)$

$O^{(2)}(z)$:

$O^{(3)}(z)$:

Hybrid-Ratio Scheme

Ji, *et al.* Nucl. Phys. B. 964:115311 (2021)

- The hybrid-ratio scheme is a renormalization scheme which handles the linear divergence from the Wilson line self energy at long distances

Hybrid-Ratio Scheme

Ji, *et al.* Nucl. Phys. B. 964:115311 (2021)

- The hybrid-ratio scheme is a renormalization scheme which handles the linear divergence from the Wilson line self energy at long distances
- We renormalize the quasi-PDF matrix elements as:

$$h^R(z, P_z) = \begin{cases} \frac{h^B(0,0)}{h^B(0,P_z)} \frac{h^B(z,P_z)}{h^B(z,0)} & z \leq z_s \\ \frac{h^B(0,0)}{h^B(0,P_z)} \frac{h^B(z,P_z)}{h^B(z_s,0)} \times e^{(\delta m + m_0)(z - z_s)} & z > z_s \end{cases}$$

Hybrid-Ratio Scheme

Ji, *et al.* Nucl. Phys. B. 964:115311 (2021)

- The hybrid-ratio scheme is a renormalization scheme which handles the linear divergence from the Wilson line self energy at long distances
- We renormalize the quasi-PDF matrix elements as:

$$h^R(z, P_z) = \begin{cases} \frac{h^B(0,0)}{h^B(0,P_z)} \frac{h^B(z,P_z)}{h^B(z,0)} & z \leq z_s \\ \frac{h^B(0,0)}{h^B(0,P_z)} \frac{h^B(z,P_z)}{h^B(z_s,0)} \times e^{(\delta m + m_0)(z - z_s)} & z > z_s \end{cases}$$

- z_s is a distance scale, before which the divergence is mostly ignorable
 - Should not be much more than ~ 0.3 fm

Hybrid-Ratio Scheme

Ji, *et al.* Nucl. Phys. B. 964:115311 (2021)

- The hybrid-ratio scheme is a renormalization scheme which handles the linear divergence from the Wilson line self energy at long distances
- We renormalize the quasi-PDF matrix elements as:

$$h^R(z, P_z) = \begin{cases} \frac{h^B(0,0)}{h^B(0,P_z)} \frac{h^B(z,P_z)}{h^B(z,0)} & z \leq z_s \\ \frac{h^B(0,0)}{h^B(0,P_z)} \frac{h^B(z,P_z)}{h^B(z_s,0)} \times e^{(\delta m + m_0)(z - z_s)} & z > z_s \end{cases}$$

- z_s is a distance scale, before which the divergence is mostly ignorable
 - Should not be much more than ~ 0.3 fm
- $\delta m + m_0$ can be fit by matching to the Wilson coefficients for the given operator

Hybrid-Ratio Scheme

Ji, *et al.* Nucl. Phys. B. 964:115311 (2021)

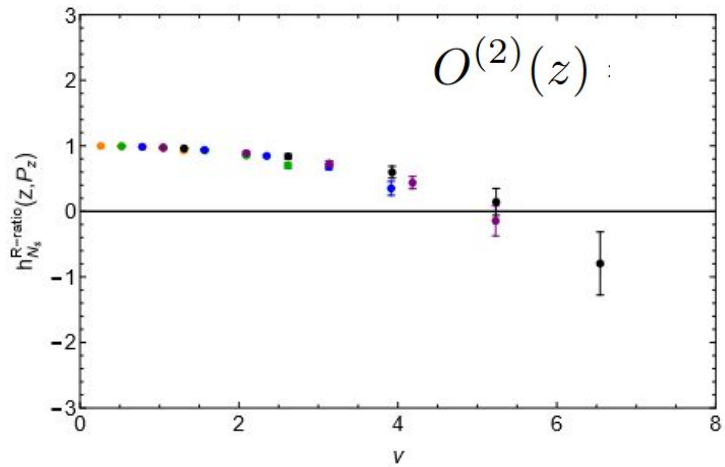
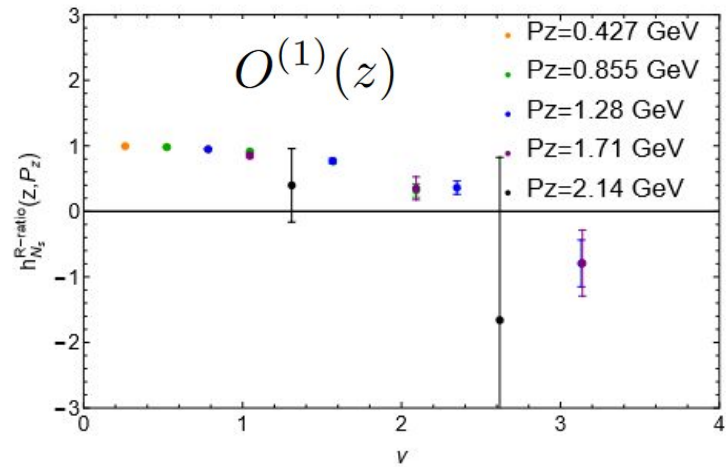
- The hybrid-ratio scheme is a renormalization scheme which handles the linear divergence from the Wilson line self energy at long distances
- We renormalize the quasi-PDF matrix elements as:

$$h^R(z, P_z) = \begin{cases} \frac{h^B(0,0)}{h^B(0,P_z)} \frac{h^B(z,P_z)}{h^B(z,0)} & z \leq z_s \\ \frac{h^B(0,0)}{h^B(0,P_z)} \frac{h^B(z,P_z)}{h^B(z_s,0)} \times e^{(\delta m + m_0)(z - z_s)} & z > z_s \end{cases}$$

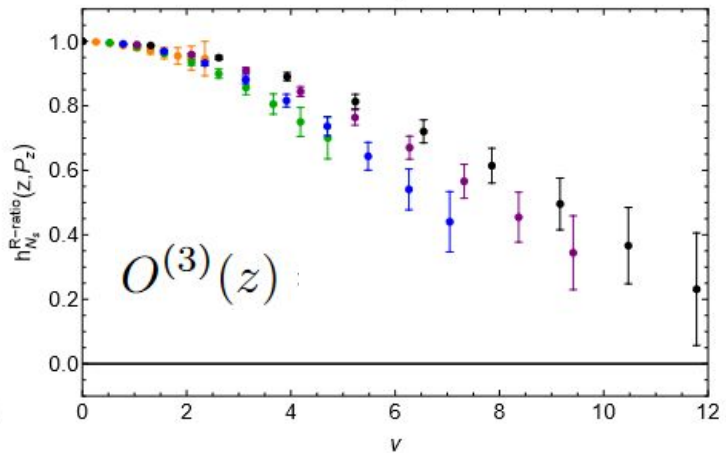
- z_s is a distance scale, before which the divergence is mostly ignorable
 - Should not be much more than ~ 0.3 fm
- $\delta m + m_0$ can be fit by matching to the Wilson coefficients for the given operator
- The hybrid-ratio scheme agrees with the standard ratio scheme for $z_s \rightarrow \infty$

Ratio Renormalized MEs $z_s \rightarrow \infty$

N_s W3

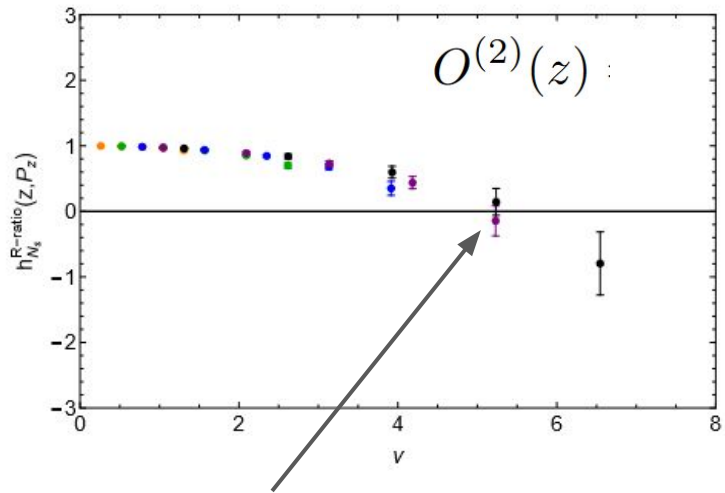
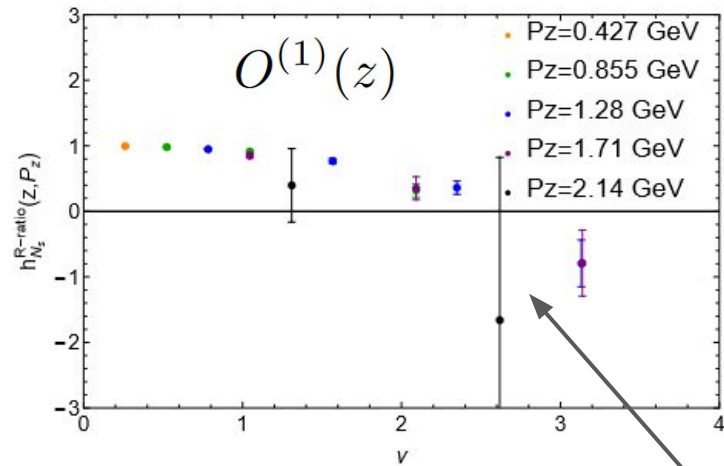


$$\nu = z P_z$$

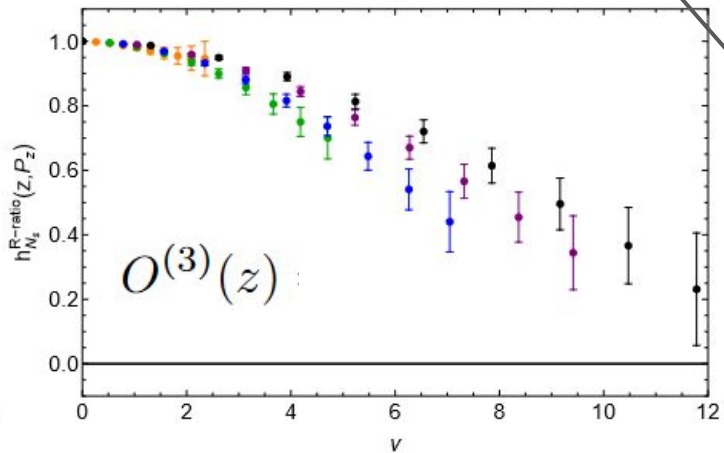


Ratio Renormalized MEs $z_s \rightarrow \infty$

N_s W3



$$\nu = zP_z$$

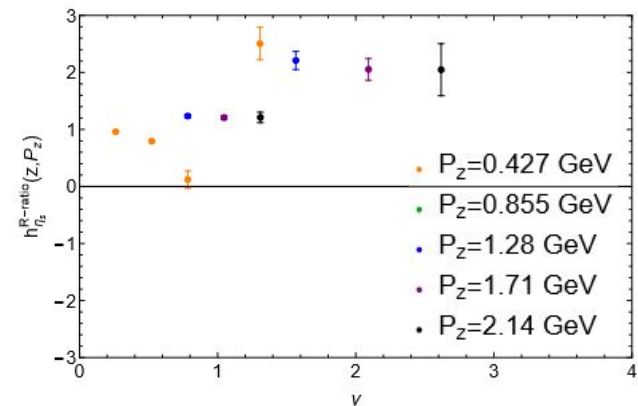


$O^{(1)}(z)$ and $O^{(2)}(z)$ both have many noisy points removed for clarity and cross zero, which is unexpected. $O^{(3)}(z)$ is much cleaner and better behaved.

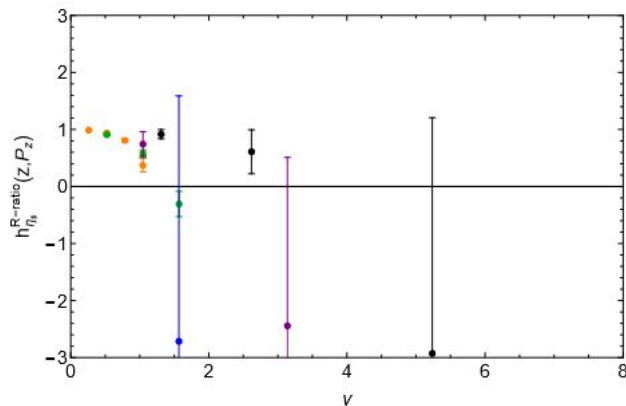
Things are Even Worse for Other Hadrons and Smearing

$\eta_s, H5$

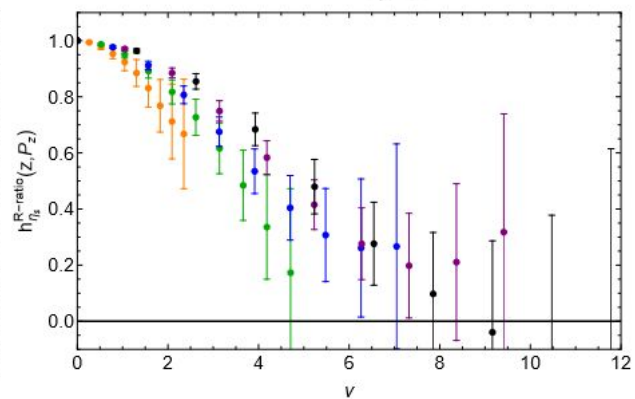
$O^{(1)}(z)$



$O^{(2)}(z)$:



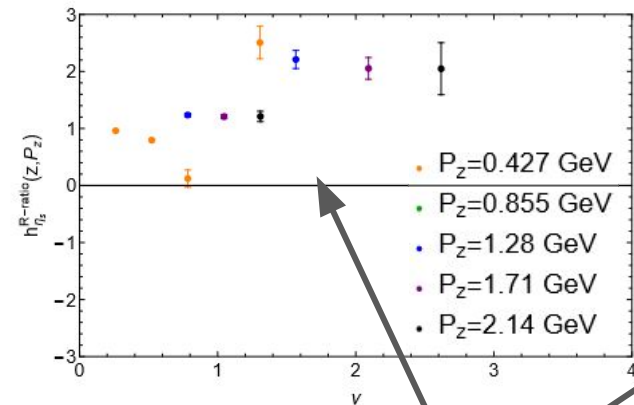
$O^{(3)}(z)$:



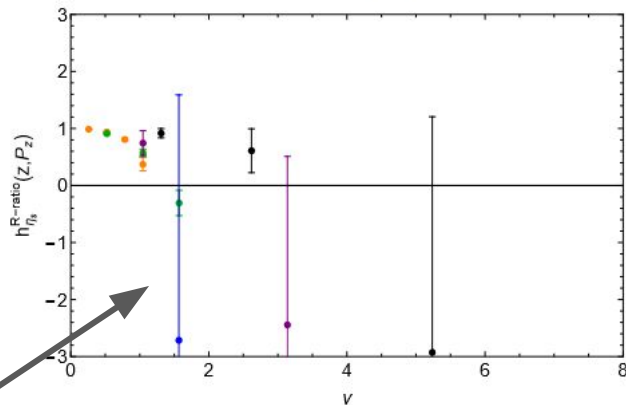
Things are Even Worse for Other Hadrons and Smearing

$\eta_s, H5$

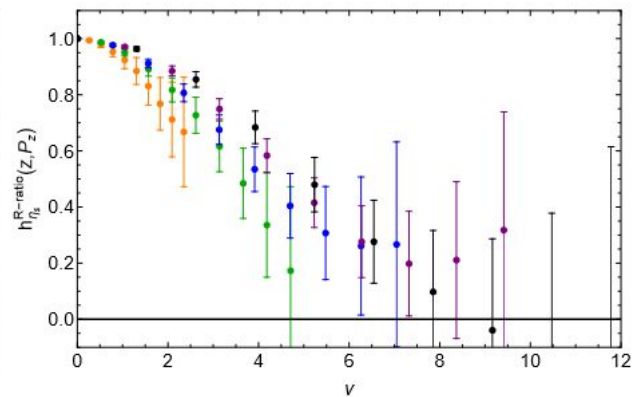
$O^{(1)}(z)$



$O^{(2)}(z)$:



$O^{(3)}(z)$:

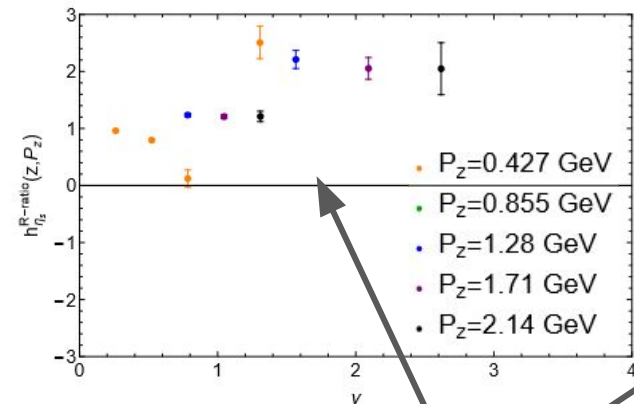


Very crazy behavior in the first two operators (likely due to zero crossings and other noise)

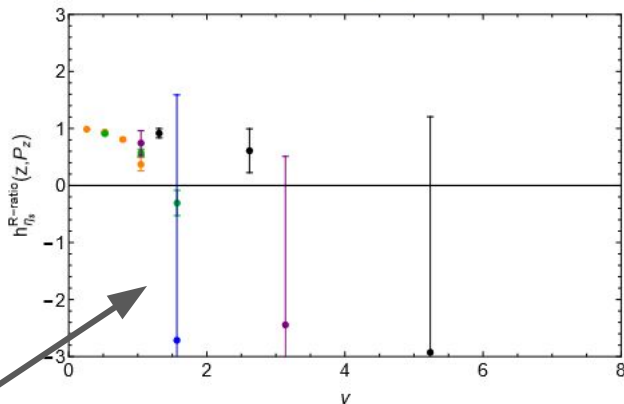
Things are Even Worse for Other Hadrons and Smearing

$\eta_s, H5$

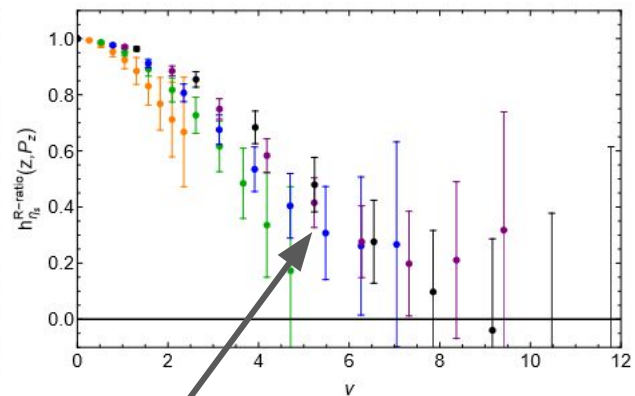
$O^{(1)}(z)$



$O^{(2)}(z)$:



$O^{(3)}(z)$:



Very crazy behavior in the first two operators (likely due to zero crossings and other noise)

Noisier, but still reasonable behavior in $O^{(3)}(z)$:

Compare to Pheno. Results

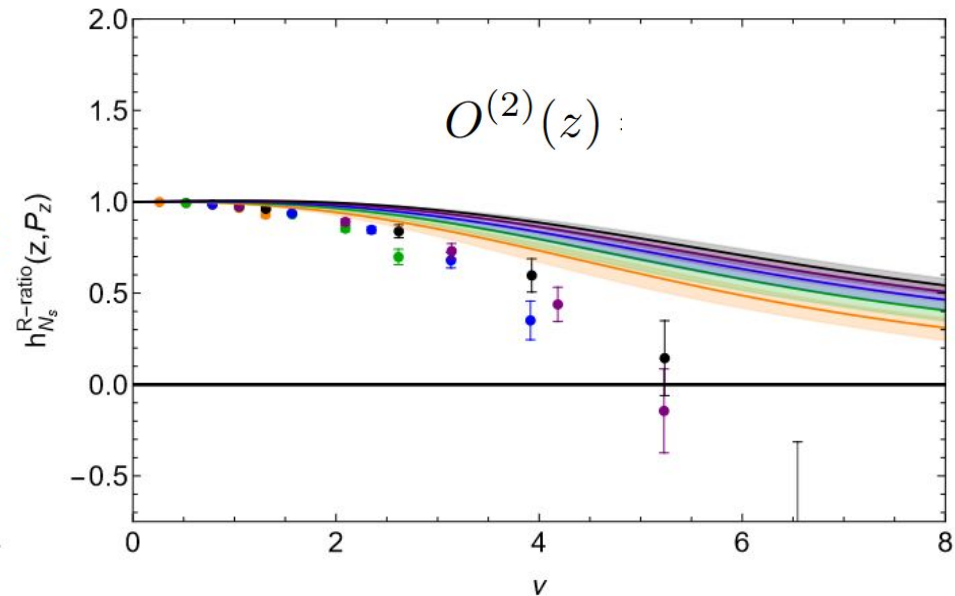
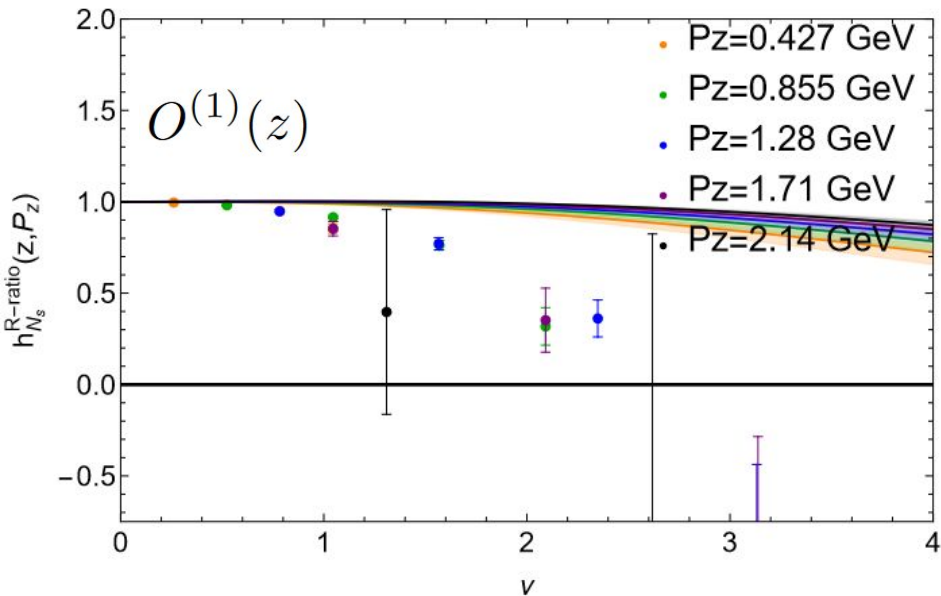
Hou *et al.* (CTEQ) PRD 103(1):014013 (2021)
Yao, *et al.* JHEP 11(2023)021

- Took the CT18 nucleon gluon PDF at $\overline{\text{MS}}$ scale $\mu = 2$ GeV to the quasi-PDF using the ratio scheme kernels and Fourier transformed to position space

Compare to Pheno. Results

Hou et al. (CTEQ) PRD 103(1):014013 (2021)
Yao, et al. JHEP 11(2023)021

- Took the CT18 nucleon gluon PDF at $\overline{\text{MS}}$ scale $\mu = 2$ GeV to the quasi-PDF using the ratio scheme kernels and Fourier transformed to position space

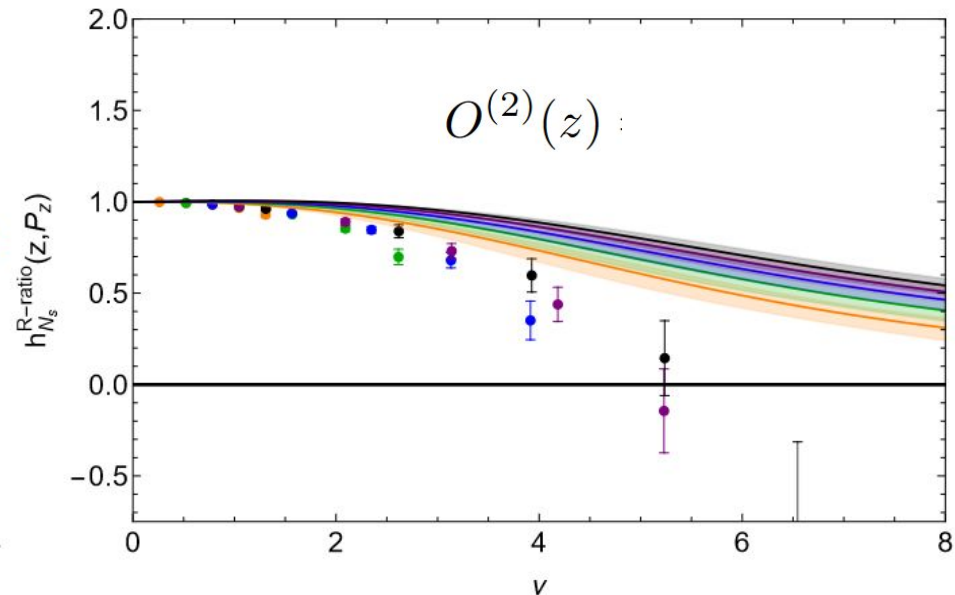
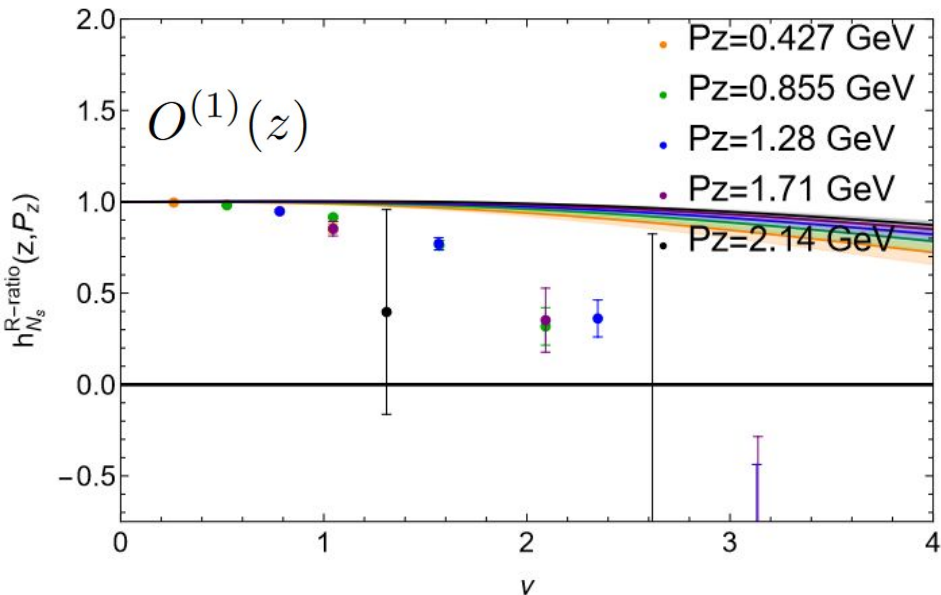


N_s W3

Compare to Pheno. Results

Hou et al. (CTEQ) PRD 103(1):014013 (2021)
Yao, et al. JHEP 11(2023)021

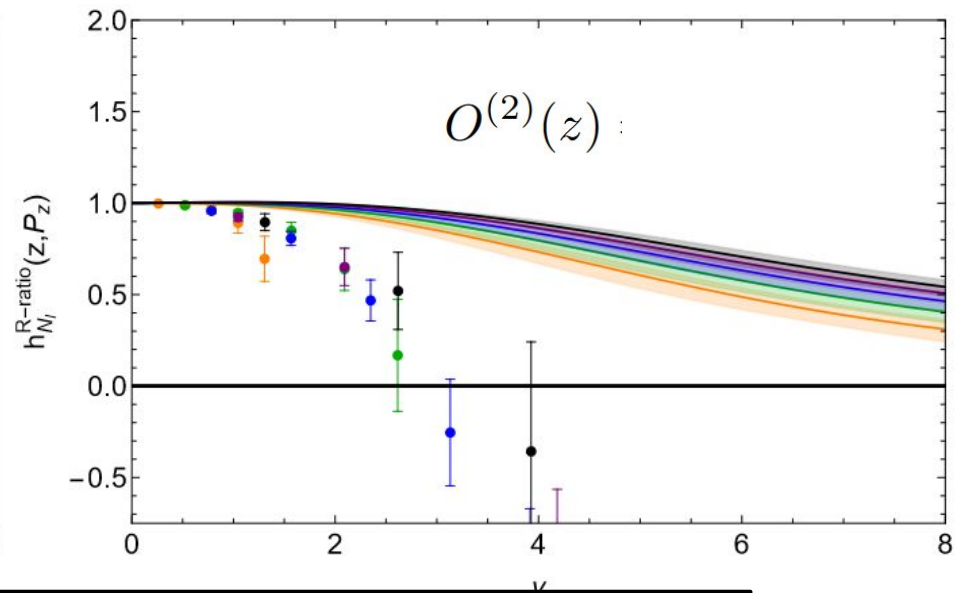
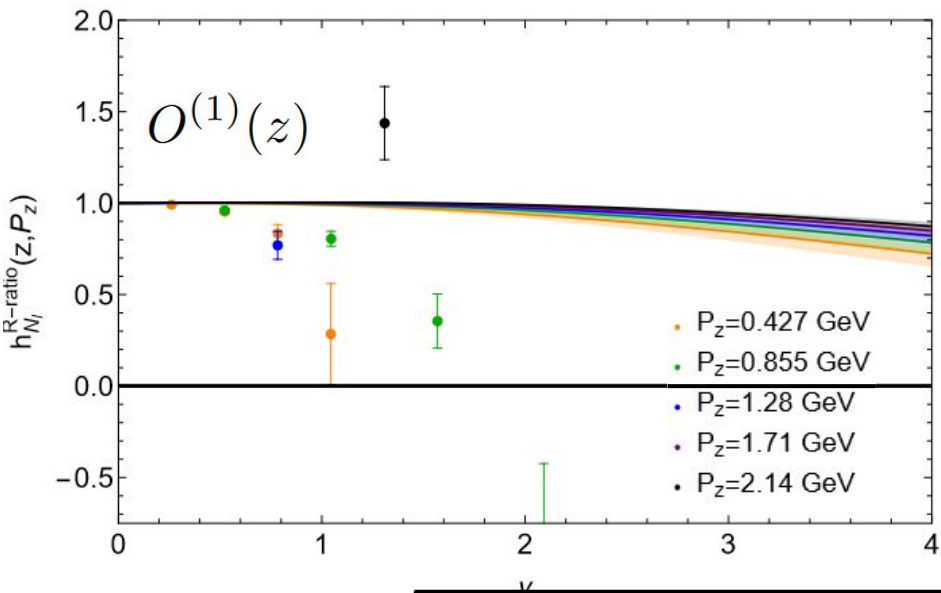
- Took the CT18 nucleon gluon PDF at $\overline{\text{MS}}$ scale $\mu = 2$ GeV to the quasi-PDF using the ratio scheme kernels and Fourier transformed to position space



N_s W3

The decay is too fast and the crossing over zero is not expected from the pheno. results

Similar Results with in H5 N_l Case

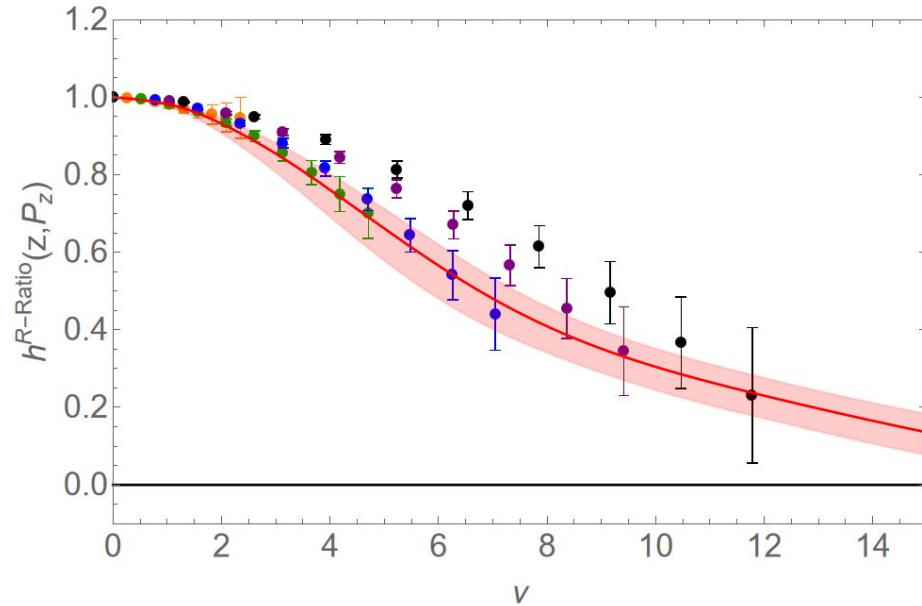


The decay and zero crossing is even worse in this case

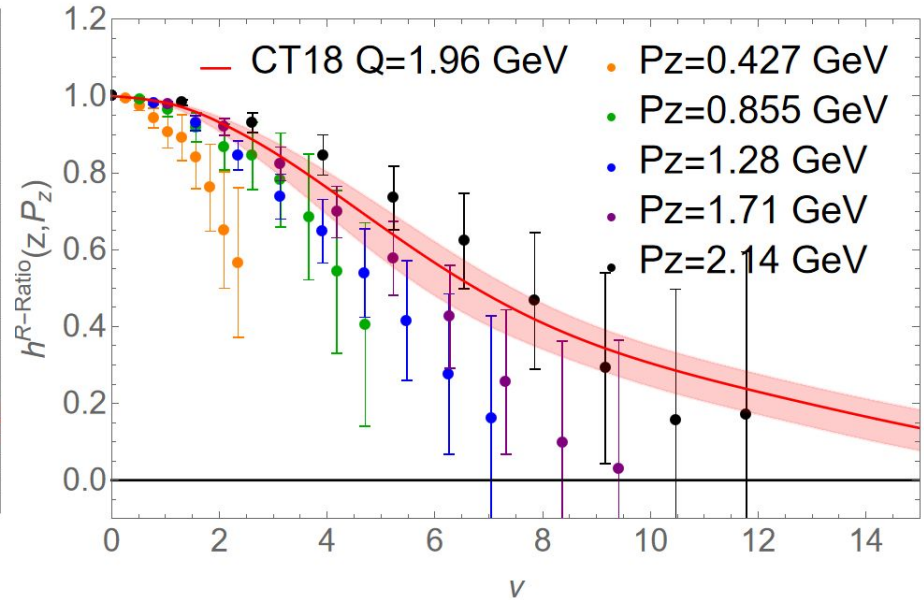
$O^{(3)}(z)$: Compared to Pheno. Matrix Elements

Hou et al. (CTEQ) PRD 103(1):014013 (2021)
Balitsky, et al., PLB 808:135621 (2020)

- Use pseudo-PDF matching kernel at $z = a$ on the same CT18 PDF



$N_s W3$



$N_l H5$

Fitting $\delta m + m_0$

Ji, *et al.* Nucl. Phys. B. 964:115311 (2021)
Gao, *et al.* PRL 128:142003 (2022)
Zhang, *et al.* PLB 844:128081 (2023)
Hou, *et al.* (LPC) Nucl. Phys. B. 969:115443 (2021)

- We essentially fit the discrepancy between the matrix elements with the Wilson coefficient at short distances to a linear model to obtain $\delta m + m_0$

$$(\delta m + m_0)z - I_0 \approx \ln [\mathcal{H}(z, \mu)/h^{\text{B}}(z, 0)]$$

Fitting $\delta m + m_0$

Ji, *et al.* Nucl. Phys. B. 964:115311 (2021)
Gao, *et al.* PRL 128:142003 (2022)
Zhang, *et al.* PLB 844:128081 (2023)
Hou, *et al.* (LPC) Nucl. Phys. B. 969:115443 (2021)

- We essentially fit the discrepancy between the matrix elements with the Wilson coefficient at short distances to a linear model to obtain $\delta m + m_0$

$$(\delta m + m_0)z - I_0 \approx \ln [\mathcal{H}(z, \mu)/h^B(z, 0)]$$

- The Wilson coefficient is a perturbative expression which is operator dependent

$$\mathcal{H}^{(i)}(0, \mu^2 z^2) = 1 + \frac{\alpha_s}{2\pi} C_A \left(-A^{(i)} L_z + B^{(i)} \right)$$

with

$$L_z = \ln \left(\frac{4e^{-2\gamma_E}}{\mu^2 z^2} \right) \quad \begin{array}{ll} A^{(1)} = \frac{11}{6} & B^{(1)} = 4 \\ A^{(2)} = \frac{11}{6} & B^{(2)} = \frac{14}{3} \end{array}$$

Fitting $\delta m + m_0$

Ji, *et al.* Nucl. Phys. B. 964:115311 (2021)
Gao, *et al.* PRL 128:142003 (2022)
Zhang, *et al.* PLB 844:128081 (2023)
Hou, *et al.* (LPC) Nucl. Phys. B. 969:115443 (2021)

- We essentially fit the discrepancy between the matrix elements with the Wilson coefficient at short distances to a linear model to obtain $\delta m + m_0$

$$(\delta m + m_0)z - I_0 \approx \ln [\mathcal{H}(z, \mu)/h^B(z, 0)]$$

- The Wilson coefficient is a perturbative expression which is operator dependent

$$\mathcal{H}^{(i)}(0, \mu^2 z^2) = 1 + \frac{\alpha_s}{2\pi} C_A \left(-A^{(i)} L_z + B^{(i)} \right)$$

with

$$L_z = \ln \left(\frac{4e^{-2\gamma_E}}{\mu^2 z^2} \right) \quad \begin{array}{ll} A^{(1)} = \frac{11}{6} & B^{(1)} = 4 \\ A^{(2)} = \frac{11}{6} & B^{(2)} = \frac{14}{3} \end{array}$$

- μ is the renormalization scale and γ_E is the Euler-Mascheroni constant

Fitting $\delta m + m_0$

Ji, et al. Nucl. Phys. B. 964:115311 (2021)
Gao, et al. PRL 128:142003 (2022)
Zhang, et al. PLB 844:128081 (2023)
Hou, et al. (LPC) Nucl. Phys. B. 969:115443 (2021)

- We essentially fit the discrepancy between the matrix elements with the Wilson coefficient at short distances to a linear model to obtain $\delta m + m_0$

$$(\delta m + m_0)z - I_0 \approx \ln [\mathcal{H}(z, \mu)/h^B(z, 0)]$$

- The Wilson coefficient is a perturbative expression which is operator dependent

$$\mathcal{H}^{(i)}(0, \mu^2 z^2) = 1 + \frac{\alpha_s}{2\pi} C_A \left(-A^{(i)} L_z + B^{(i)} \right)$$

with

$$L_z = \ln \left(\frac{4e^{-2\gamma_E}}{\mu^2 z^2} \right) \quad \begin{array}{ll} A^{(1)} = \frac{11}{6} & B^{(1)} = 4 \\ A^{(2)} = \frac{11}{6} & B^{(2)} = \frac{14}{3} \end{array}$$

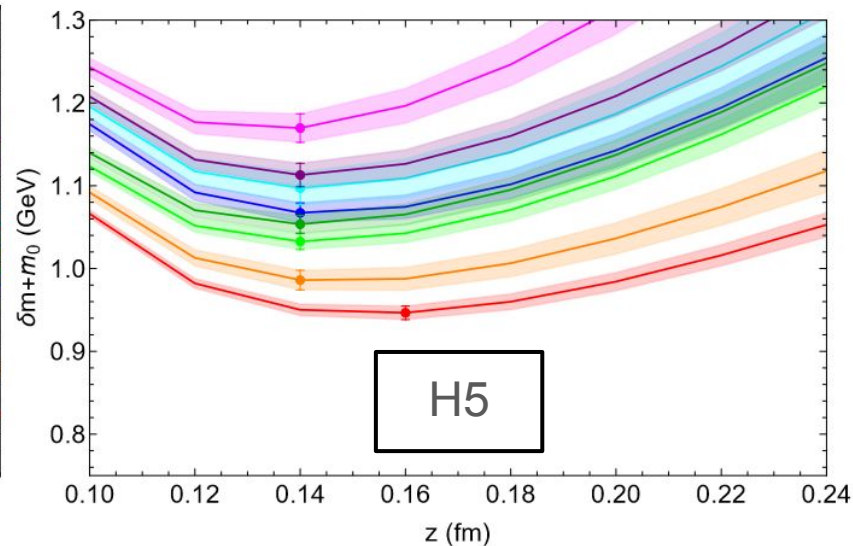
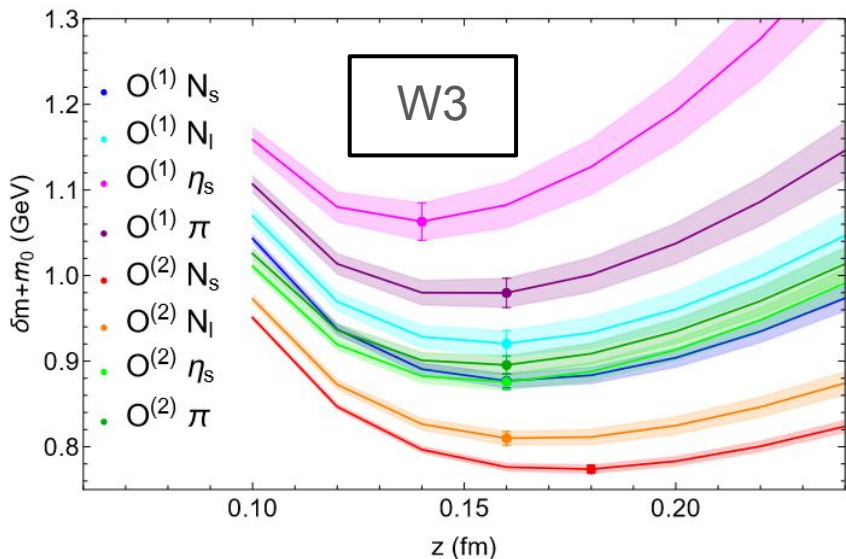
- μ is the renormalization scale and γ_E is the Euler-Mascheroni constant
- We only have the Wilson coefficients for $O^{(1)}(z)$ and $O^{(2)}(z)$:

Fit Results

- Due to the coarse lattice spacing, we interpolate the data in the small- z range. We do this, then fit to three points $\{z-0.02 \text{ fm}, z, z +0.02 \text{ fm}\}$, varying z

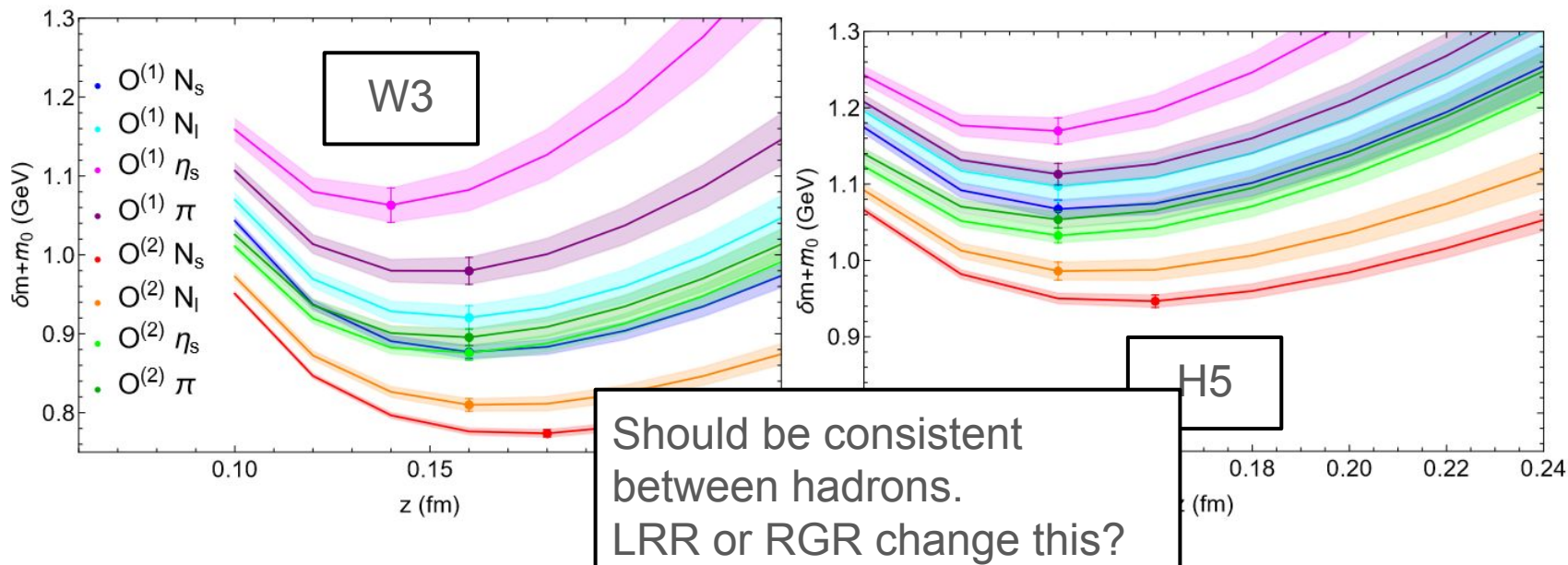
Fit Results

- Due to the coarse lattice spacing, we interpolate the data in the small- z range. We do this, then fit to three points $\{z-0.02 \text{ fm}, z, z+0.02 \text{ fm}\}$, varying z
- We compare each operator and hadron



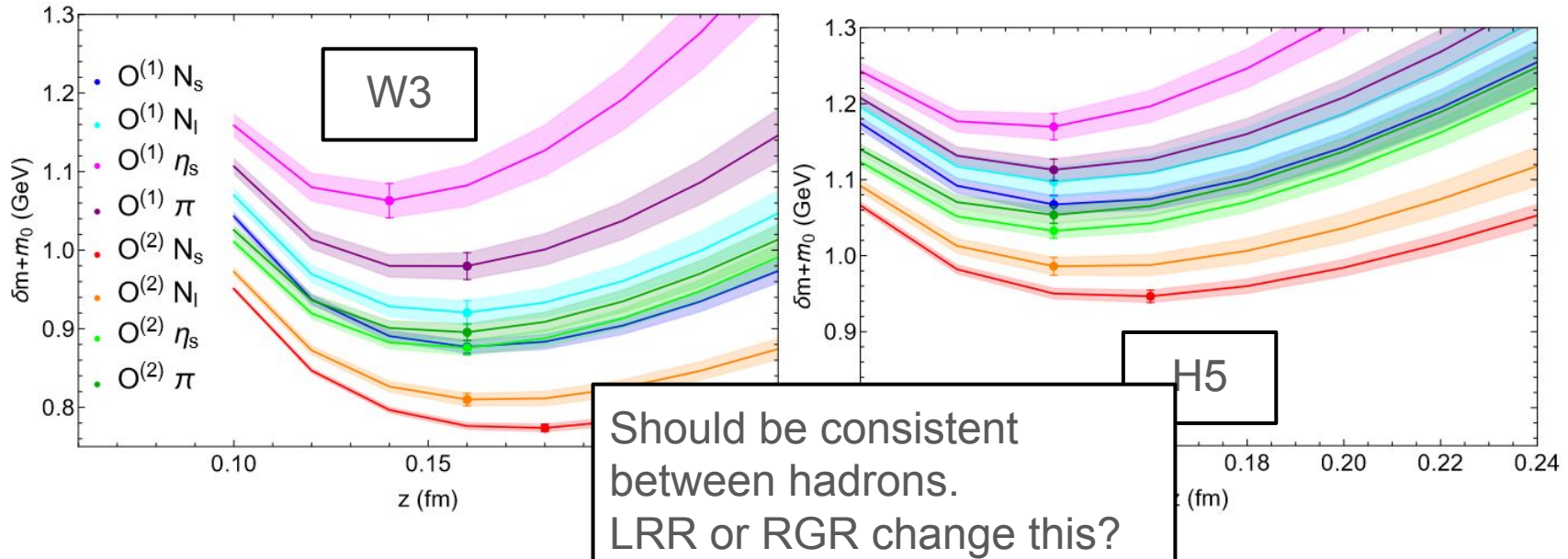
Fit Results

- Due to the coarse lattice spacing, we interpolate the data in the small- z range. We do this, then fit to three points $\{z-0.02 \text{ fm}, z, z+0.02 \text{ fm}\}$, varying z
- We compare each operator and hadron

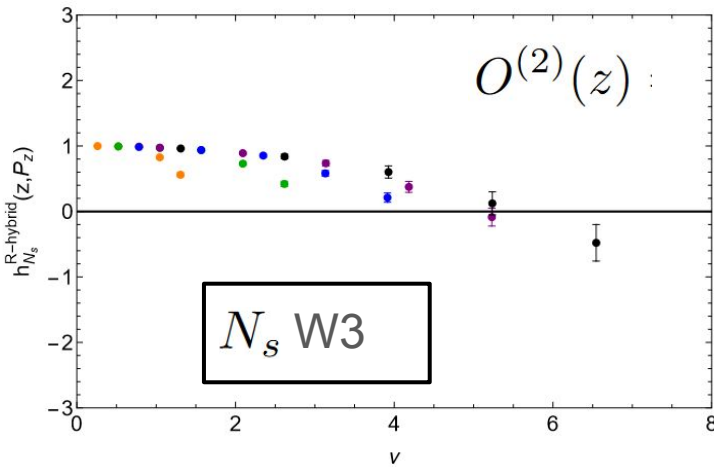
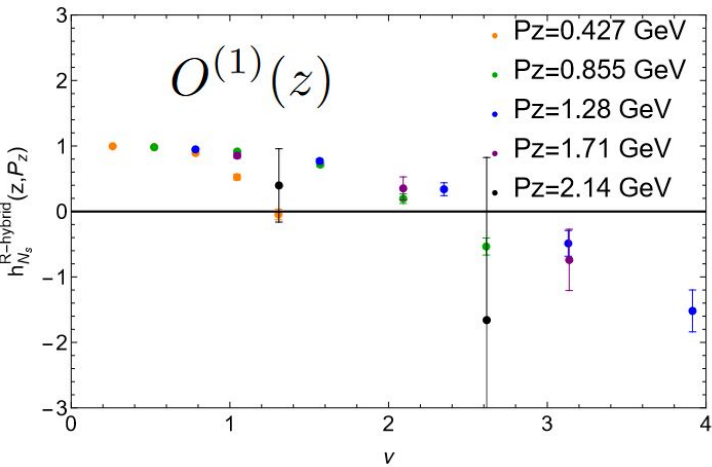


Fit Results

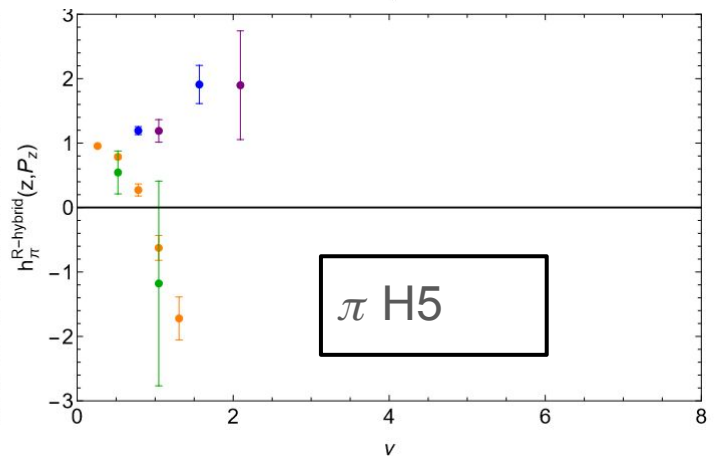
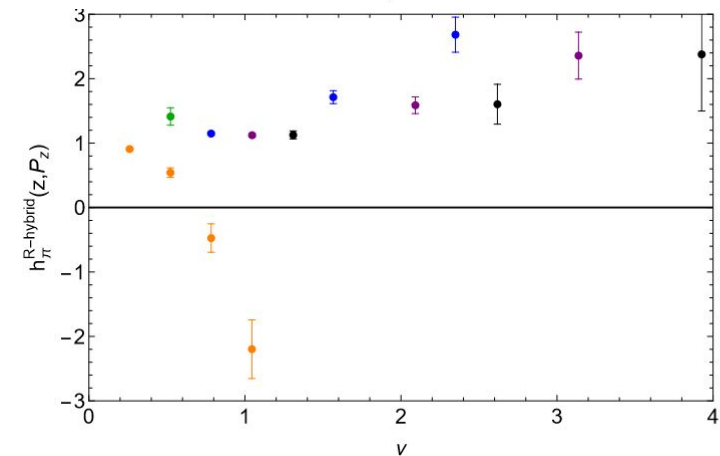
- Due to the coarse lattice spacing, we interpolate the data in the small- z range. We do this, then fit to three points $\{z-0.02 \text{ fm}, z, z+0.02 \text{ fm}\}$, varying z
- We compare each operator and hadron
- We choose the minimum fitted $\delta m + m_0$ as it is typically in the most linear range of the data



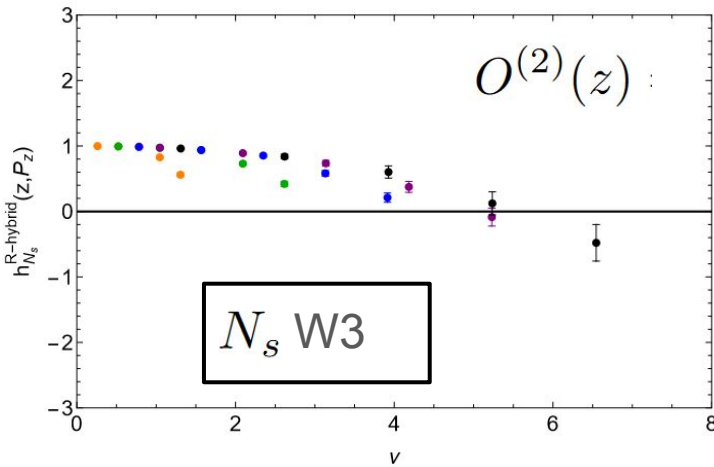
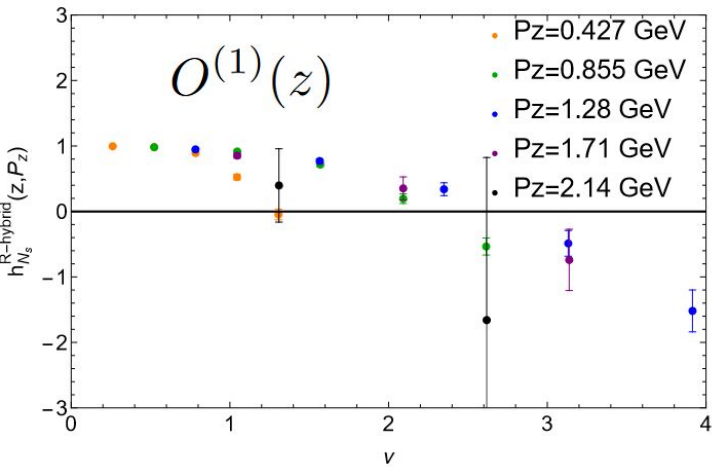
Does Hybrid Renormalization Change Anything?



$$z_s = 0.24 \text{ fm}$$



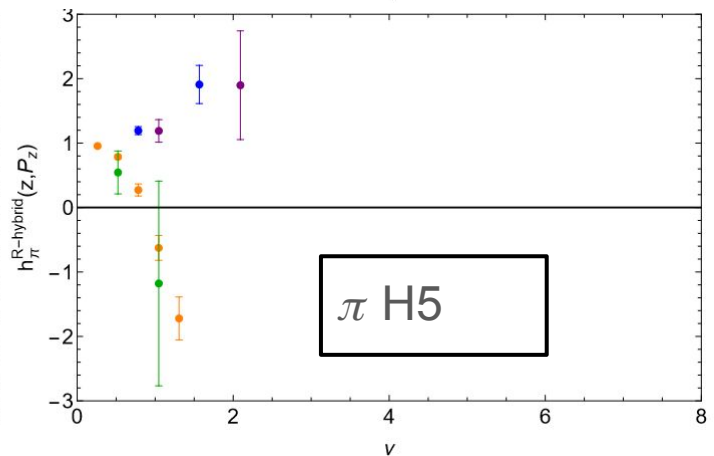
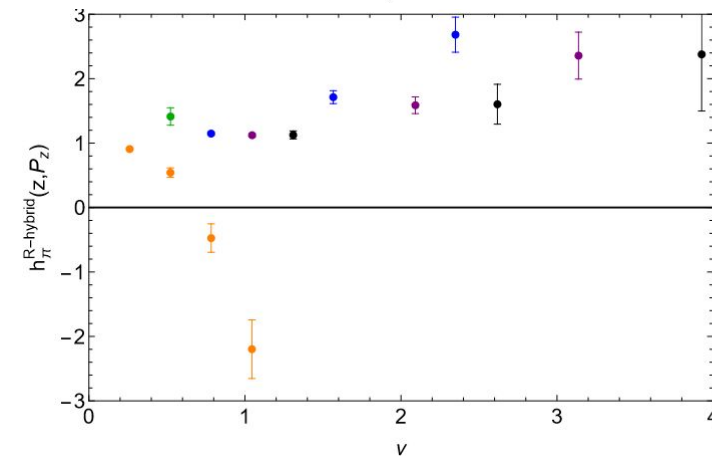
Does Hybrid Renormalization Change Anything?



$z_s = 0.24 \text{ fm}$

$N_s \text{ W3}$

With hybrid renormalization we still see zero crossings, lots of noise and divergent behavior



$\pi \text{ H5}$

Compare to Pheno. Results

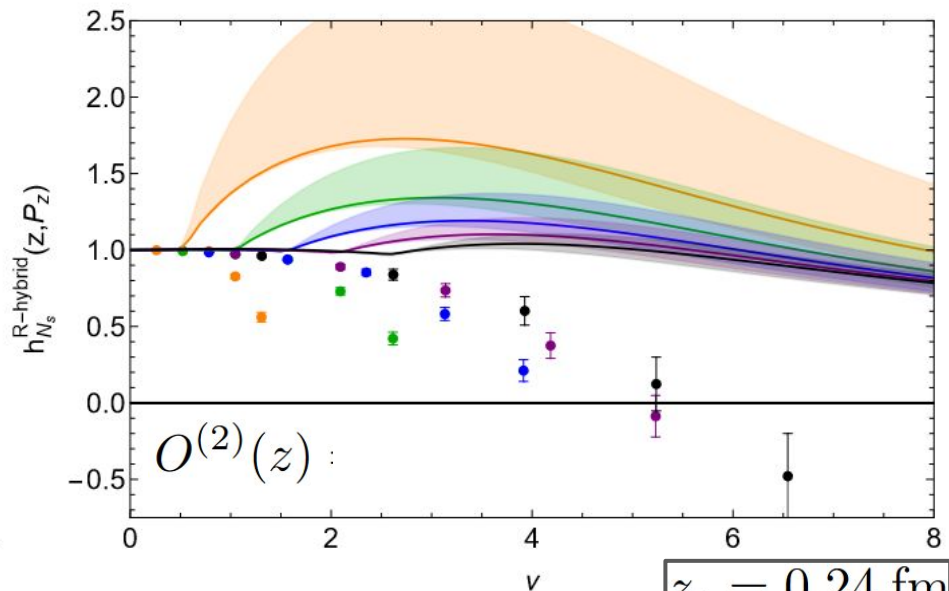
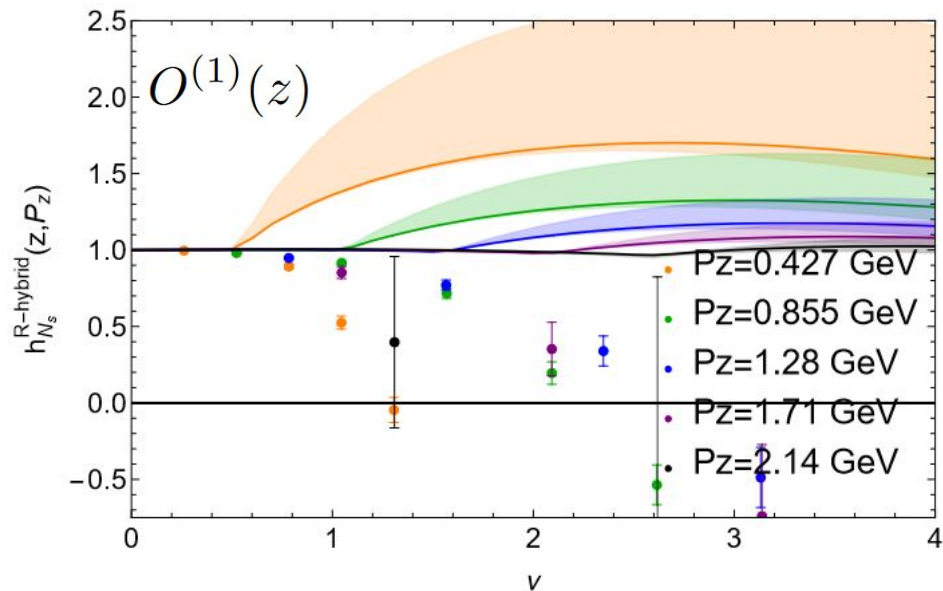
Hou *et al.* (CTEQ) PRD 103(1):014013 (2021)
Yao, *et al.* JHEP 11(2023)021

- Took the same pheno. PDF as before and transformed it similarly using the hybrid-ratio kernels and a Fourier transform to position space

Compare to Pheno. Results

Hou *et al.* (CTEQ) PRD 103(1):014013 (2021)
Yao, *et al.* JHEP 11(2023)021

- Took the same pheno. PDF as before and transformed it similarly using the hybrid-ratio kernels and a Fourier transform to position space

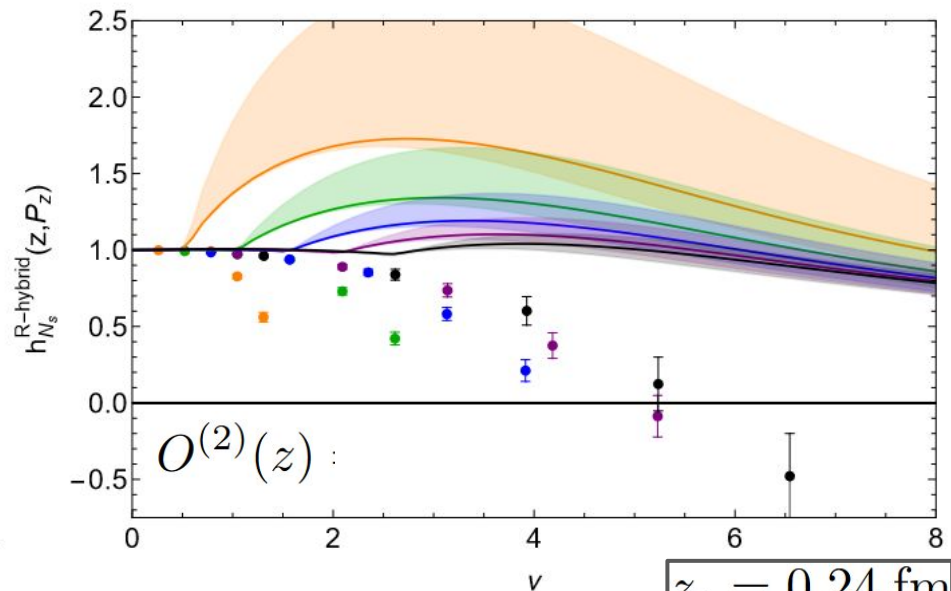
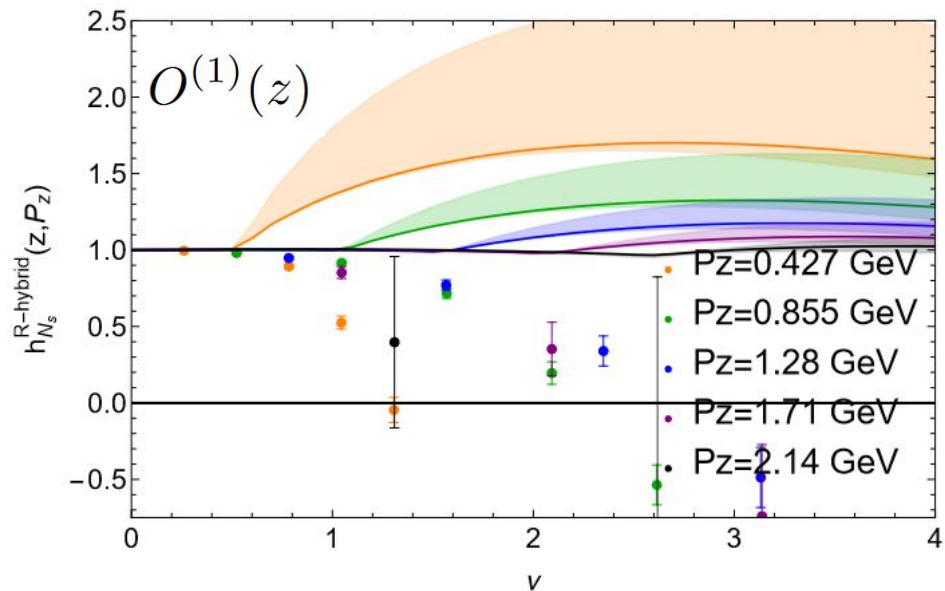


$z_s = 0.24$ fm

N_s W3

Compare to Pheno. Results

- Took the same pheno. PDF as before and transformed it similarly using the hybrid-ratio kernels and a Fourier transform to position space

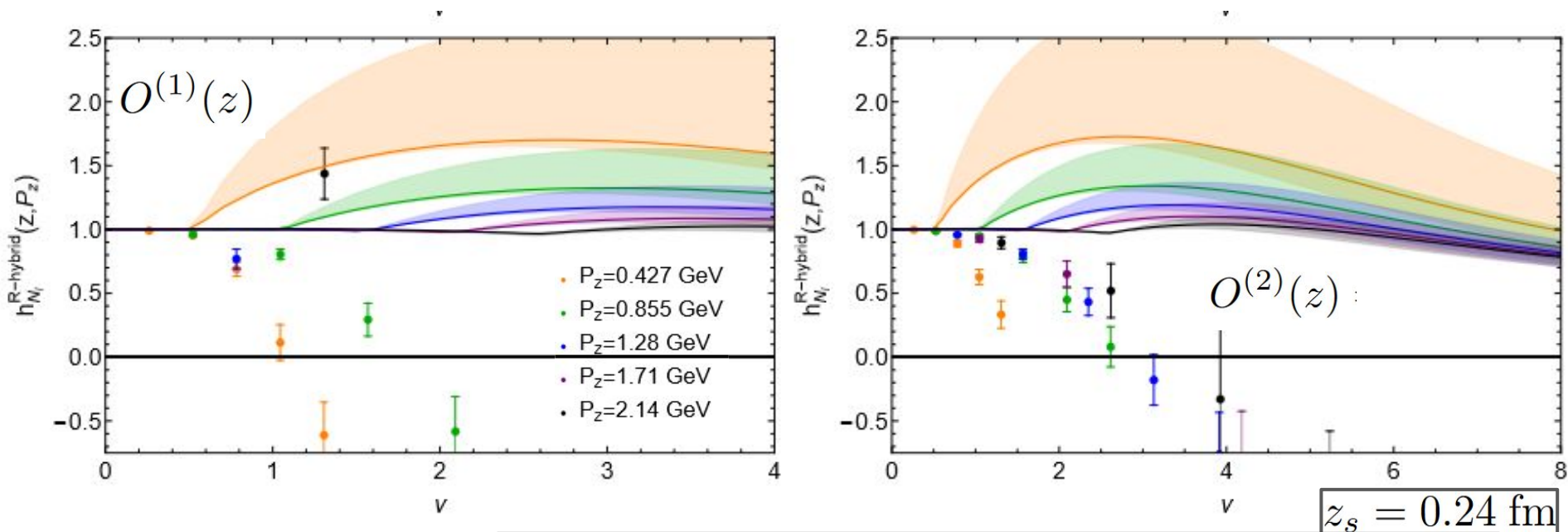


$z_s = 0.24$ fm

N_s W3

Hybrid renormalized pheno. matrix elements have a large bump and still don't capture the zero crossing

Light Nucleon Results for Hybrid-Renormalization



N_l W3

Even worse decay and divergences

$O^{(3)}(z)$ Hybrid Renormalization Guess

- We cannot get $\delta m + m_0$ fit for $O^{(3)}(z)$ as we do not have the Wilson coefficients

$O^{(3)}(z)$ Hybrid Renormalization Guess

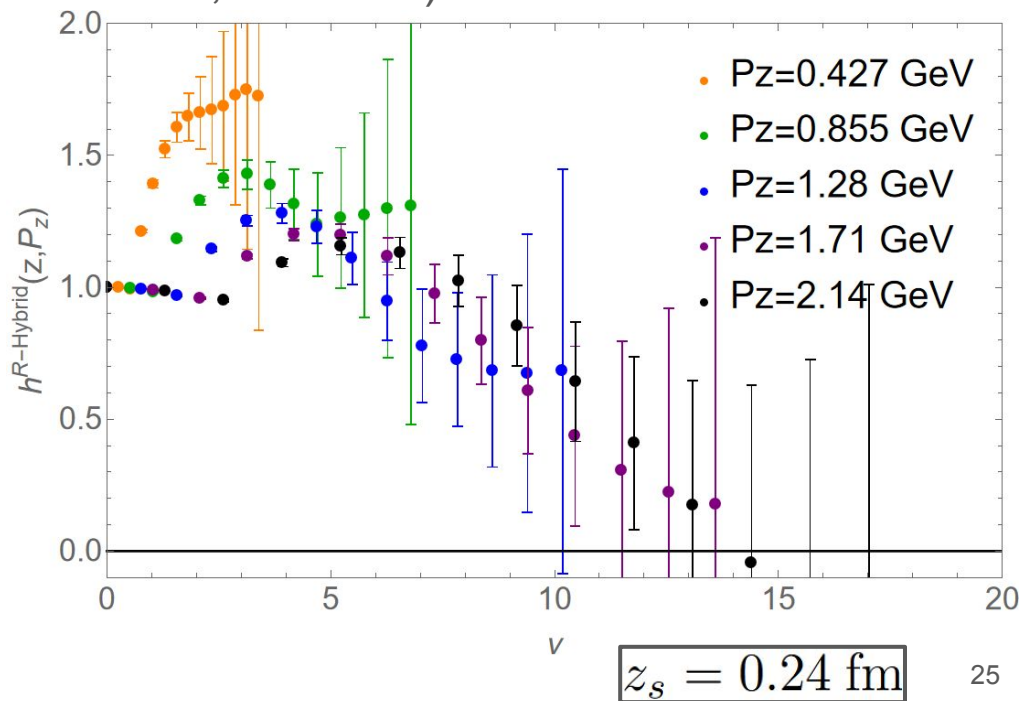
- We cannot get $\delta m + m_0$ fit for $O^{(3)}(z)$ as we do not have the Wilson coefficients
- We instead make a qualitative guess just to play out what we might see from our cleanest data (strange nucleon, Wilson-3)

$O^{(3)}(z)$ Hybrid Renormalization Guess

- We cannot get $\delta m + m_0$ fit for $O^{(3)}(z)$ as we do not have the Wilson coefficients
- We instead make a qualitative guess just to play out what we might see from our cleanest data (strange nucleon, Wilson-3)
- We pick $\delta m + m_0 = 0.65 \text{ GeV}$

$O^{(3)}(z)$ Hybrid Renormalization Guess

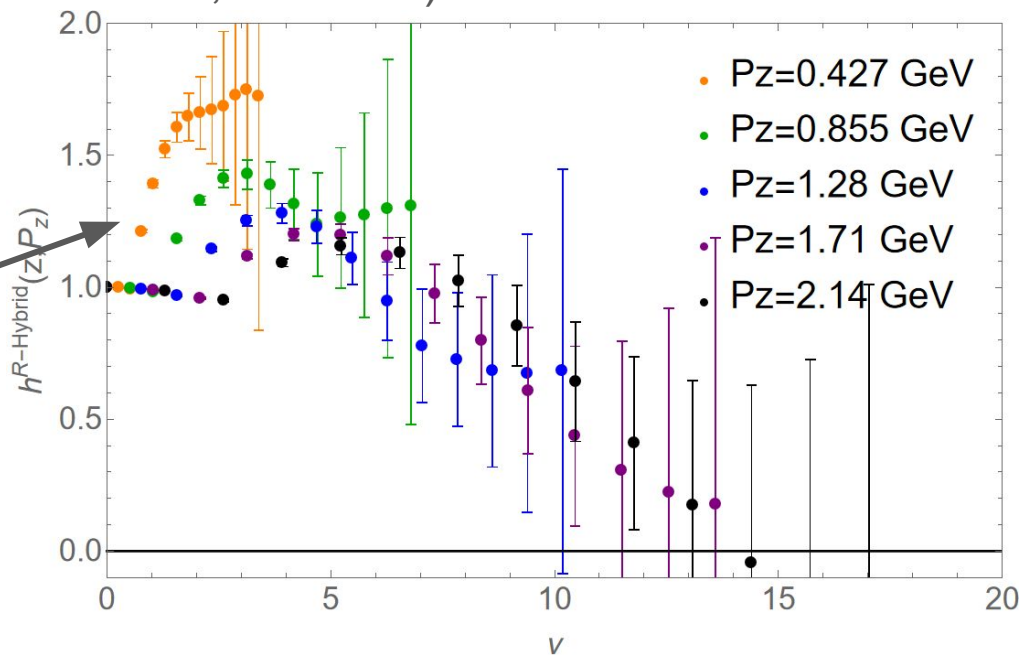
- We cannot get $\delta m + m_0$ fit for $O^{(3)}(z)$ as we do not have the Wilson coefficients
- We instead make a qualitative guess just to play out what we might see from our cleanest data (strange nucleon, Wilson-3)
- We pick $\delta m + m_0 = 0.65$ GeV and plot the hybrid-ratio renormalized matrix element *guess*



$O^{(3)}(z)$ Hybrid Renormalization Guess

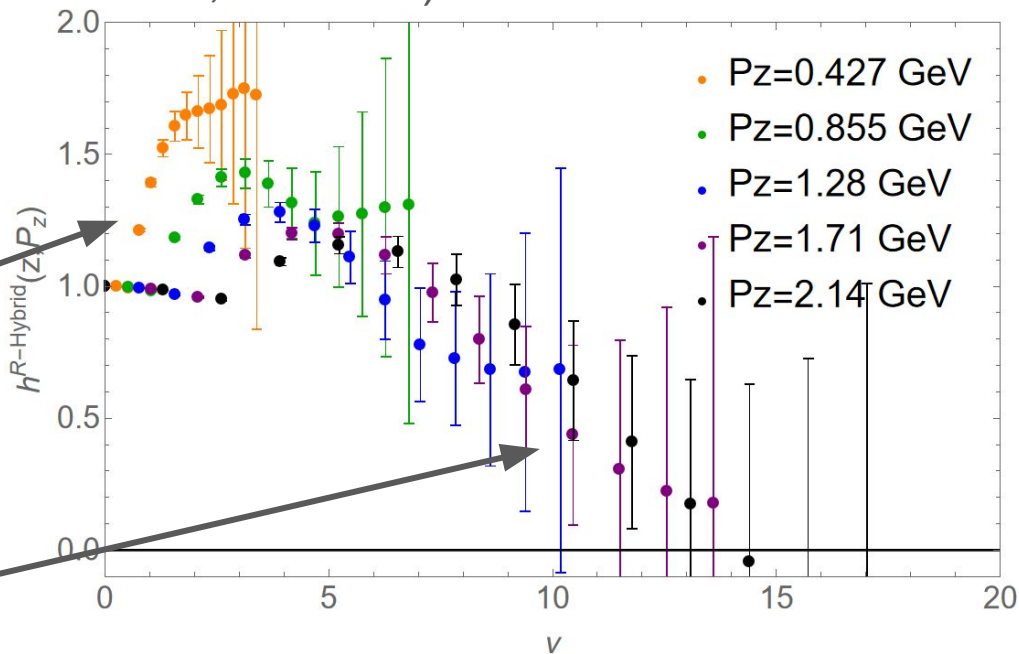
- We cannot get $\delta m + m_0$ fit for $O^{(3)}(z)$ as we do not have the Wilson coefficients
- We instead make a qualitative guess just to play out what we might see from our cleanest data (strange nucleon, Wilson-3)
- We pick $\delta m + m_0 = 0.65$ GeV and plot the hybrid-ratio renormalized matrix element *guess*

Bump after ν_s as seen in pheno. results



$O^{(3)}(z)$ Hybrid Renormalization Guess

- We cannot get $\delta m + m_0$ fit for $O^{(3)}(z)$ as we do not have the Wilson coefficients
- We instead make a qualitative guess just to play out what we might see from our cleanest data (strange nucleon, Wilson-3)
- We pick $\delta m + m_0 = 0.65$ GeV and plot the hybrid-ratio renormalized matrix element *guess*



Bump after ν_s as seen in pheno. results

Reasonable signal and seemingly nice decay for $P_z = 1.71$ GeV. Let's follow this and see what happens

Extrapolating to Large ν

- We have to extrapolate to larger ν to be able to Fourier transform our imaging of the hybrid-ratio renormalized $O^{(3)}(z)$ matrix elements

Extrapolating to Large ν

- We have to extrapolate to larger ν to be able to Fourier transform our imaging of the hybrid-ratio renormalized $O^{(3)}(z)$ matrix elements

- We use large distance form, with A, m, d as fit parameters $h^R(z, P_z) \approx A \frac{e^{-m\nu}}{|\nu|^d}$

Extrapolating to Large ν

- We have to extrapolate to larger ν to be able to Fourier transform our imaging of the hybrid-ratio renormalized $O^{(3)}(z)$ matrix elements

- We use large distance form, with A, m, d as fit parameters $h^R(z, P_z) \approx A \frac{e^{-m\nu}}{|\nu|^d}$

- Fit data in range $z=9a-13a$

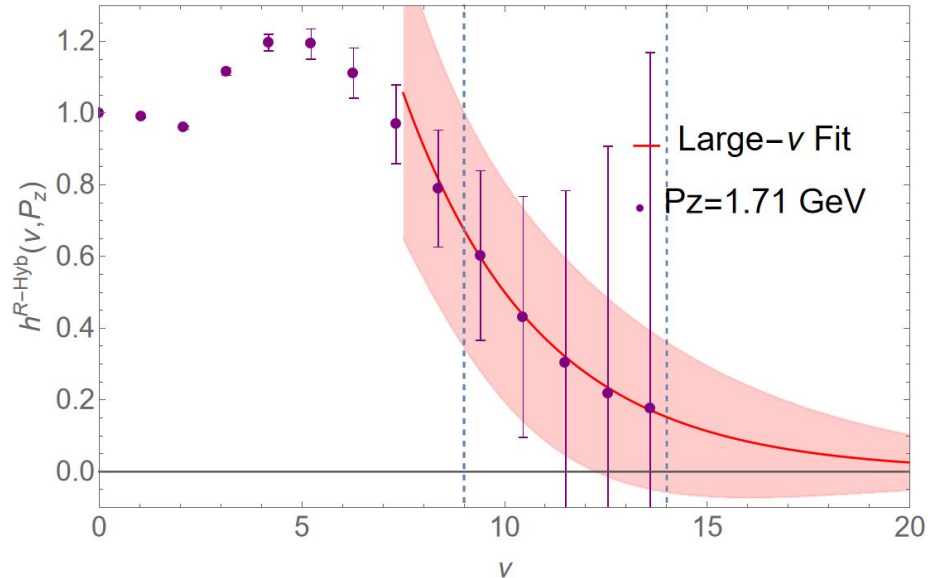
Extrapolating to Large ν

- We have to extrapolate to larger ν to be able to Fourier transform our imagining of the hybrid-ratio renormalized $O^{(3)}(z)$ matrix elements

- We use large distance form, with A, m, d as fit parameters $h^R(z, P_z) \approx A \frac{e^{-m\nu}}{|\nu|^d}$

- Fit data in range $z=9a-13a$

- The error of the fit is pretty large, but it is smaller than the error in the data at large distances



Extrapolating to Large ν

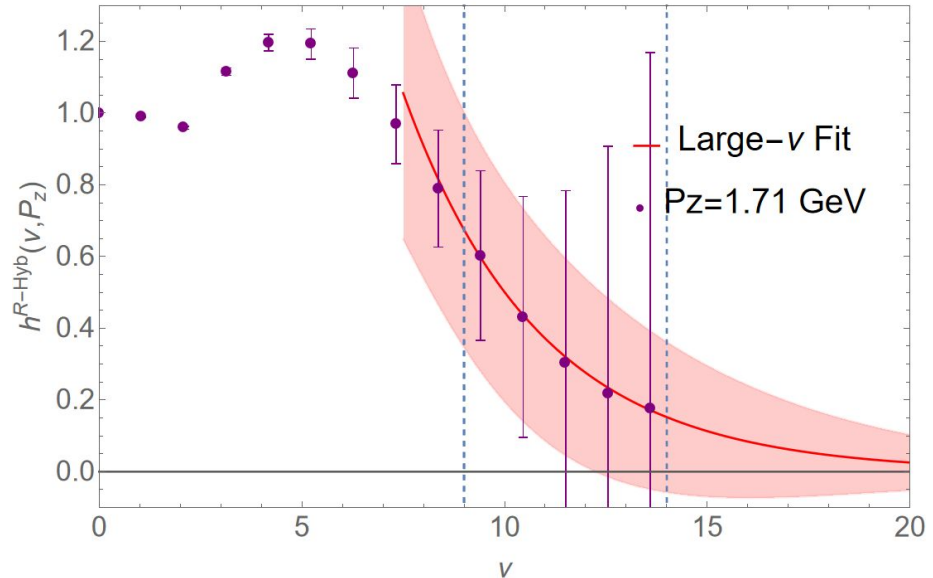
- We have to extrapolate to larger ν to be able to Fourier transform our imaging of the hybrid-ratio renormalized $O^{(3)}(z)$ matrix elements

- We use large distance form, with A, m, d as fit parameters $h^R(z, P_z) \approx A \frac{e^{-m\nu}}{|\nu|^d}$

- Fit data in range $z=9a-13a$

- The error of the fit is pretty large, but it is smaller than the error in the data at large distances

- Let's keep following this



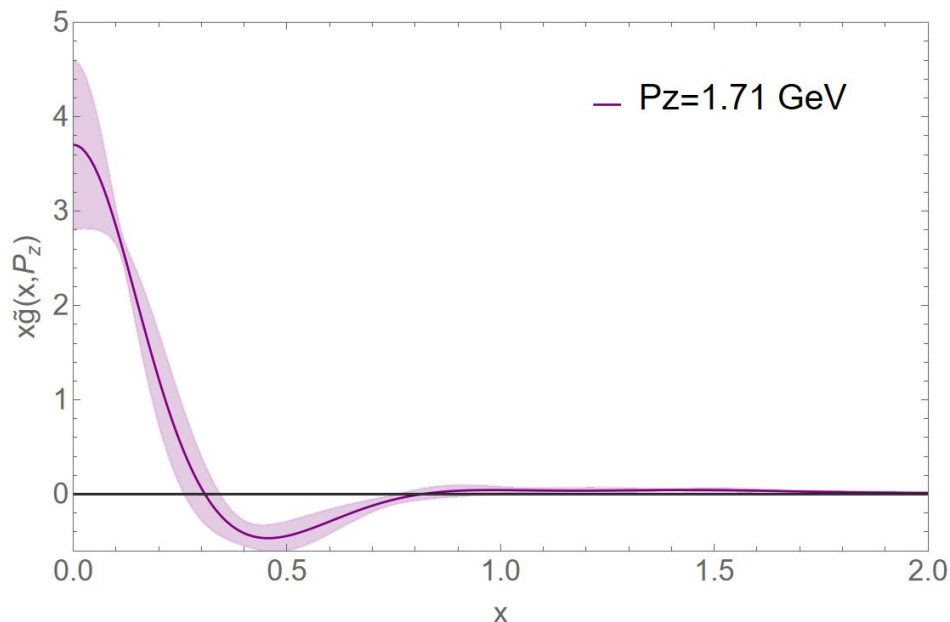
The Imagined Gluon Quasi-PDF

- We interpolate the small- ν data and use the extrapolation after around $\nu=10$ in order to get a Fourier transform of the matrix elements, giving us the first* nucleon gluon quasi-PDF from lattice data

*Relies on a guess for the critical $\delta m + m_0$ value in hybrid renormalization

The Imagined Gluon Quasi-PDF

- We interpolate the small- ν data and use the extrapolation after around $\nu=10$ in order to get a Fourier transform of the matrix elements, giving us the first* nucleon gluon quasi-PDF from lattice data

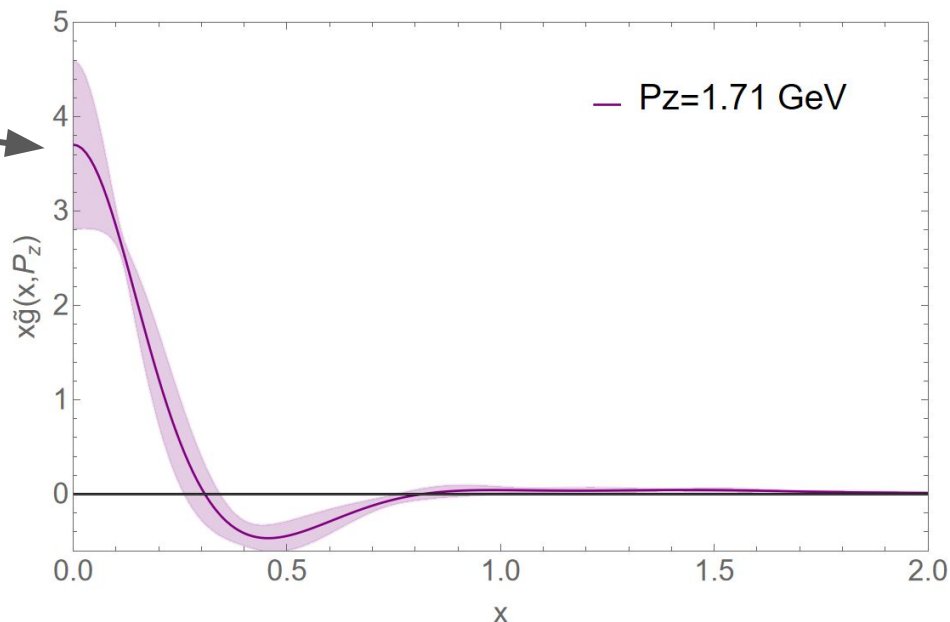


*Relies on a guess for the critical $\delta m + m_0$ value in hybrid renormalization

The Imagined Gluon Quasi-PDF

- We interpolate the small- ν data and use the extrapolation after around $\nu=10$ in order to get a Fourier transform of the matrix elements, giving us the first* nucleon gluon quasi-PDF from lattice data

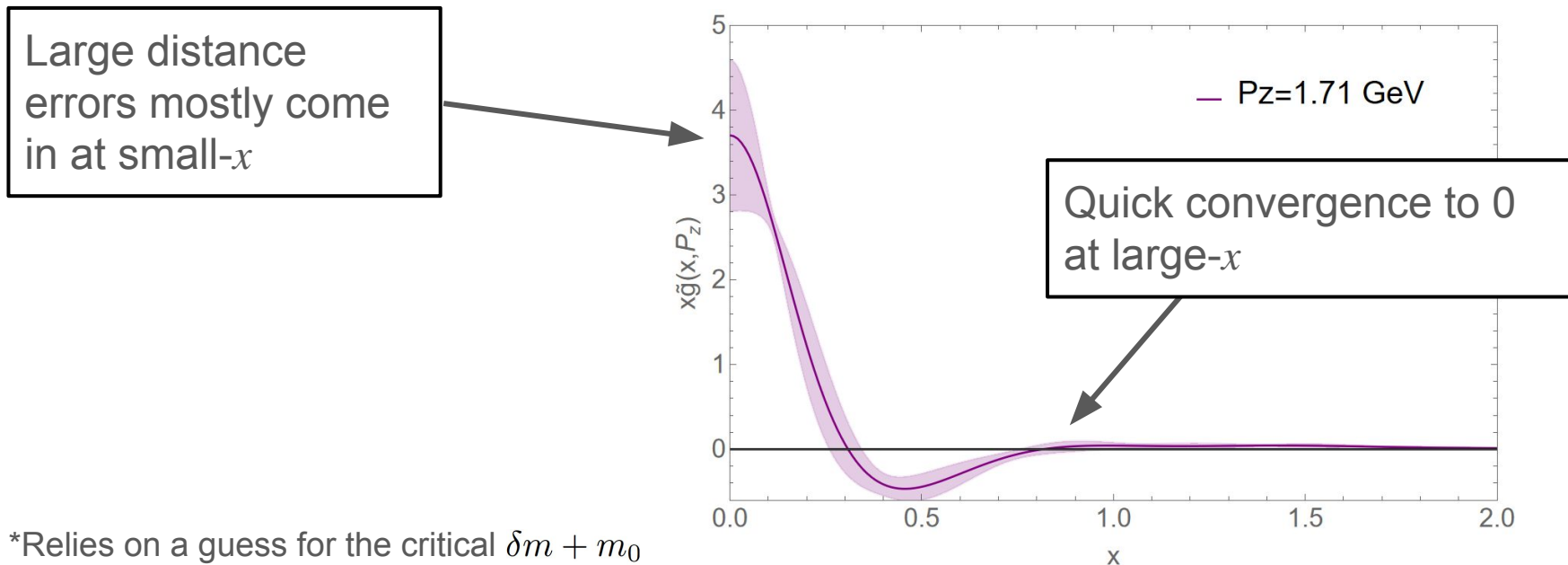
Large distance errors mostly come in at small- x



*Relies on a guess for the critical $\delta m + m_0$ value in hybrid renormalization

The Imagined Gluon Quasi-PDF

- We interpolate the small- ν data and use the extrapolation after around $\nu=10$ in order to get a Fourier transform of the matrix elements, giving us the first* nucleon gluon quasi-PDF from lattice data



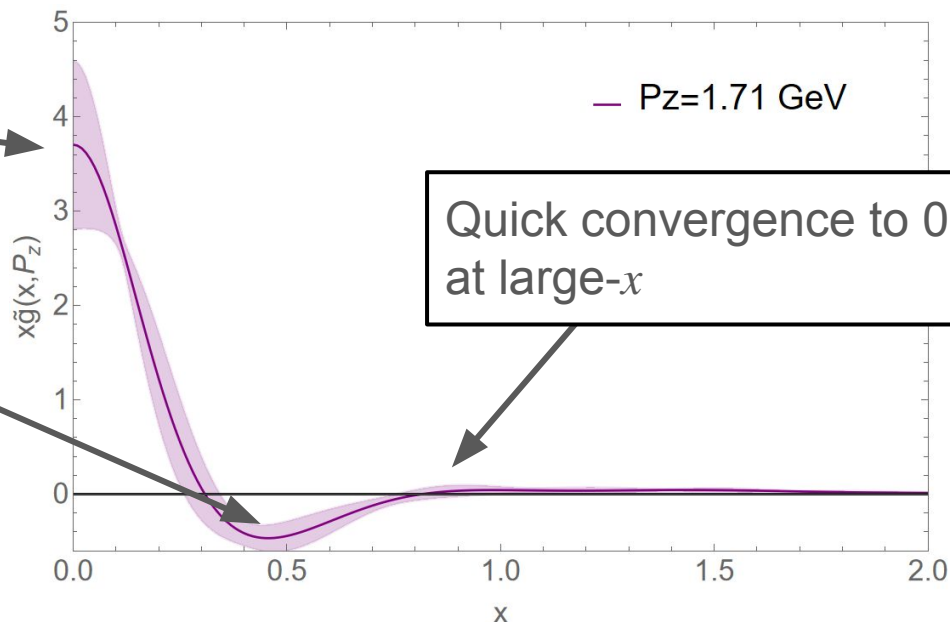
*Relies on a guess for the critical $\delta m + m_0$ value in hybrid renormalization

The Imagined Gluon Quasi-PDF

- We interpolate the small- ν data and use the extrapolation after around $\nu=10$ in order to get a Fourier transform of the matrix elements, giving us the first* nucleon gluon quasi-PDF from lattice data

Large distance errors mostly come in at small- x

Dip below zero (hopefully this would go away with real hybrid-renorm. or when matching to the light-cone)



Quick convergence to 0 at large- x

*Relies on a guess for the critical $\delta m + m_0$ value in hybrid renormalization

Coulomb Gauge Fixing

- It is clear that even in the $O^{(3)}(z)$ case, that we need to find a way to reduce the statistical noise of the measurements to push to larger distances

Coulomb Gauge Fixing

- It is clear that even in the $O^{(3)}(z)$ case, that we need to find a way to reduce the statistical noise of the measurements to push to larger distances
- We wish to explore the recent idea of removing the Wilson line from the operator and fixing to the Coulomb gauge (CG)

Coulomb Gauge Fixing

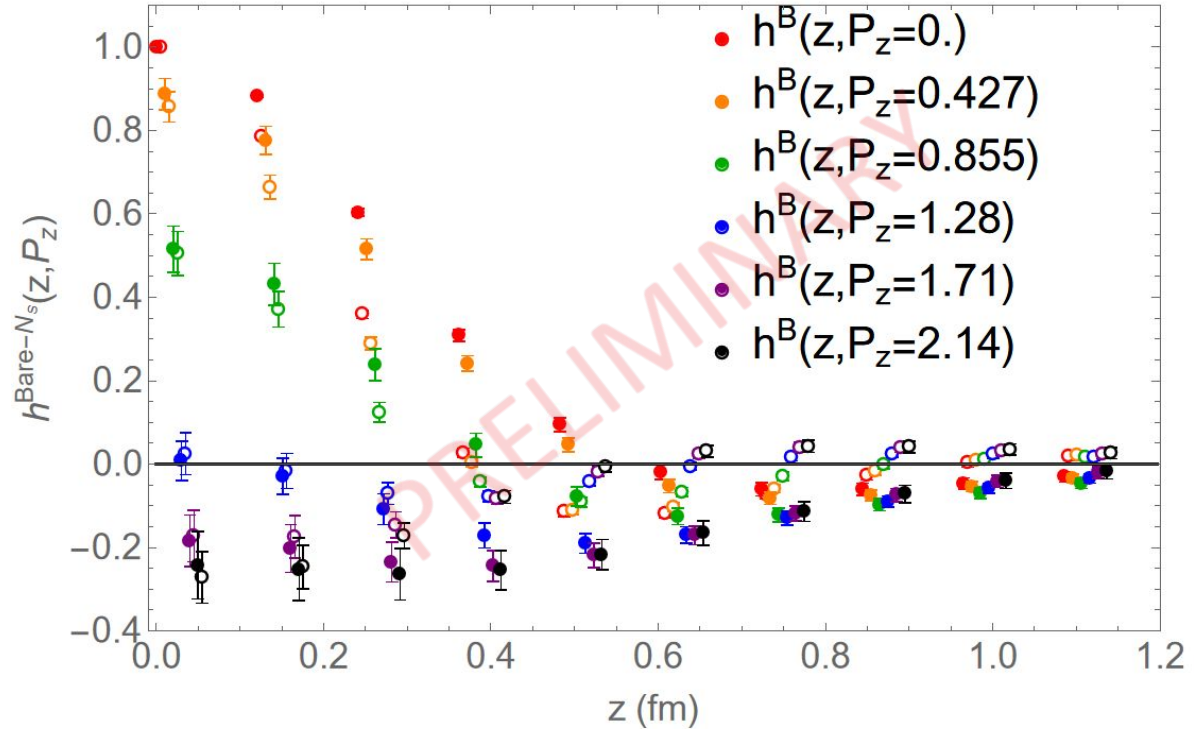
- It is clear that even in the $O^{(3)}(z)$ case, that we need to find a way to reduce the statistical noise of the measurements to push to larger distances
- We wish to explore the recent idea of removing the Wilson line from the operator and fixing to the Coulomb gauge (CG)
- After smearing, we implement gauge fixing with a precision of 10^{-7} for the calculation of the gluon loops

Coulomb Gauge Fixing

- It is clear that even in the $O^{(3)}(z)$ case, that we need to find a way to reduce the statistical noise of the measurements to push to larger distances
- We wish to explore the recent idea of removing the Wilson line from the operator and fixing to the Coulomb gauge (CG)
- After smearing, we implement gauge fixing with a precision of 10^{-7} for the calculation of the gluon loops
- As a first look, we only consider the strange nucleon with Wilson-3 smearing for $O^{(1)}(z)$

Bare Matrix Elements

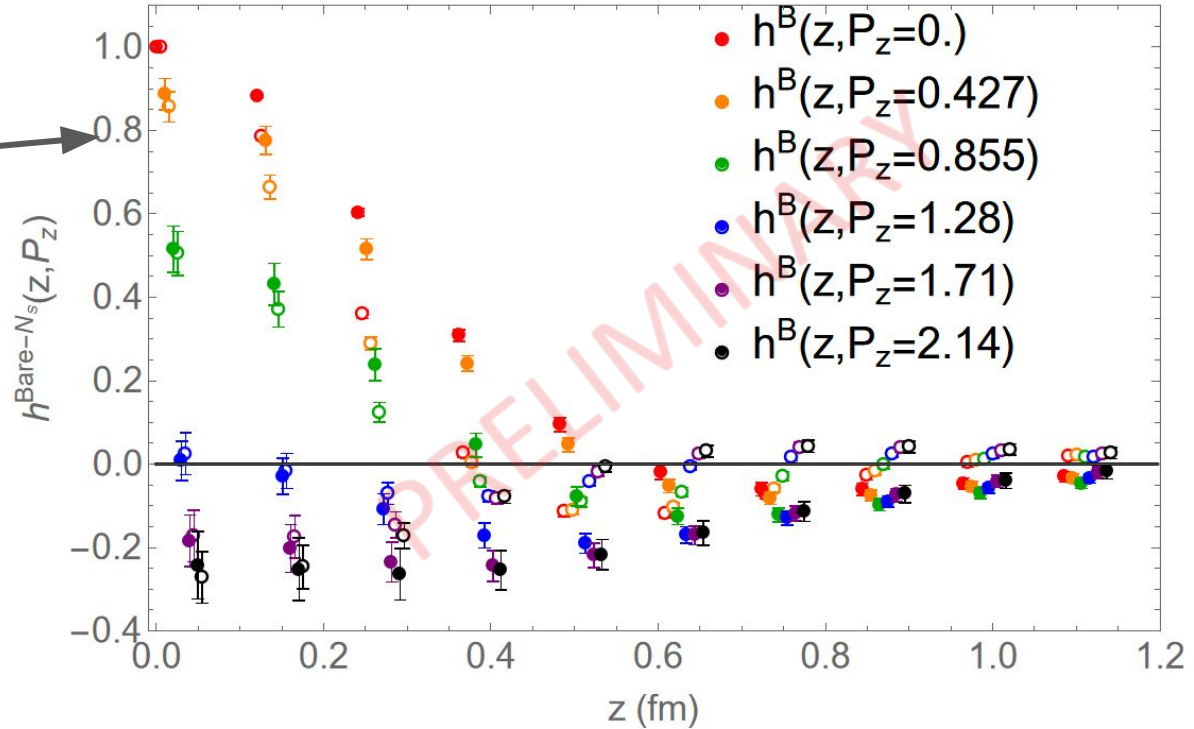
- Bare CG (open circles) and gauge invariant (GI) (closed circles) matrix elements:



Bare Matrix Elements

- Bare CG (open circles) and gauge invariant (GI) (closed circles) matrix elements:

Agreement with local operator

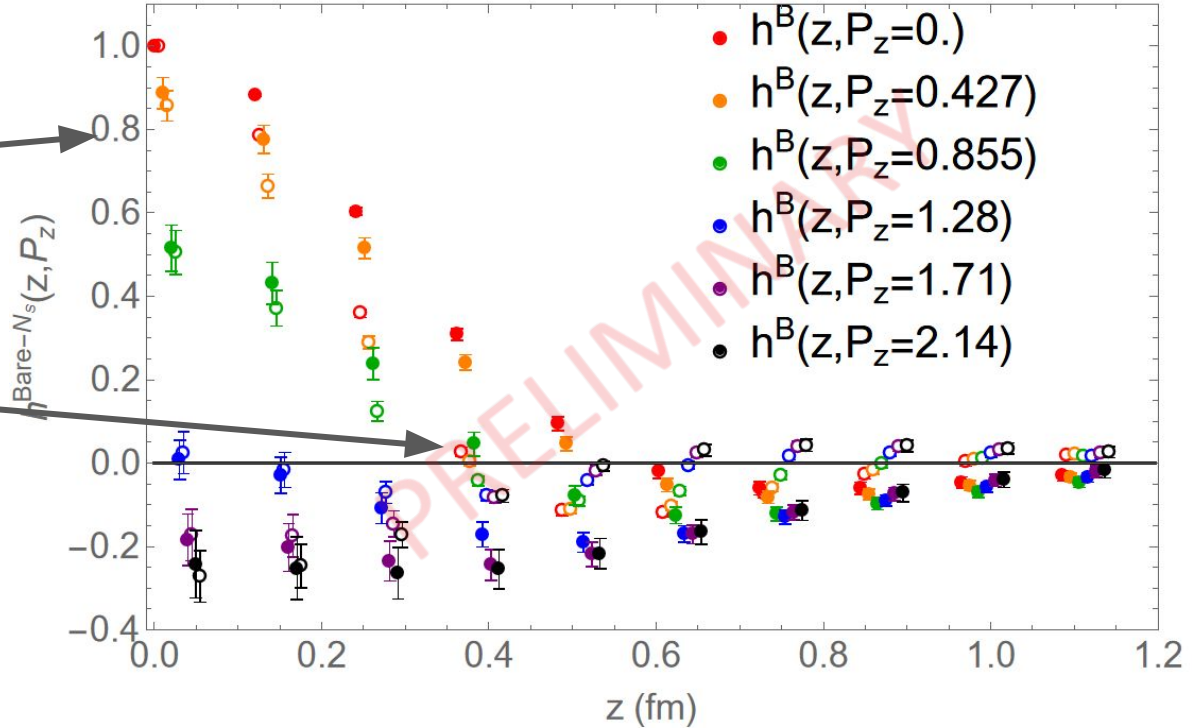


Bare Matrix Elements

- Bare CG (open circles) and gauge invariant (GI) (closed circles) matrix elements:

Agreement with local operator

More rapid decay and different zero crossing



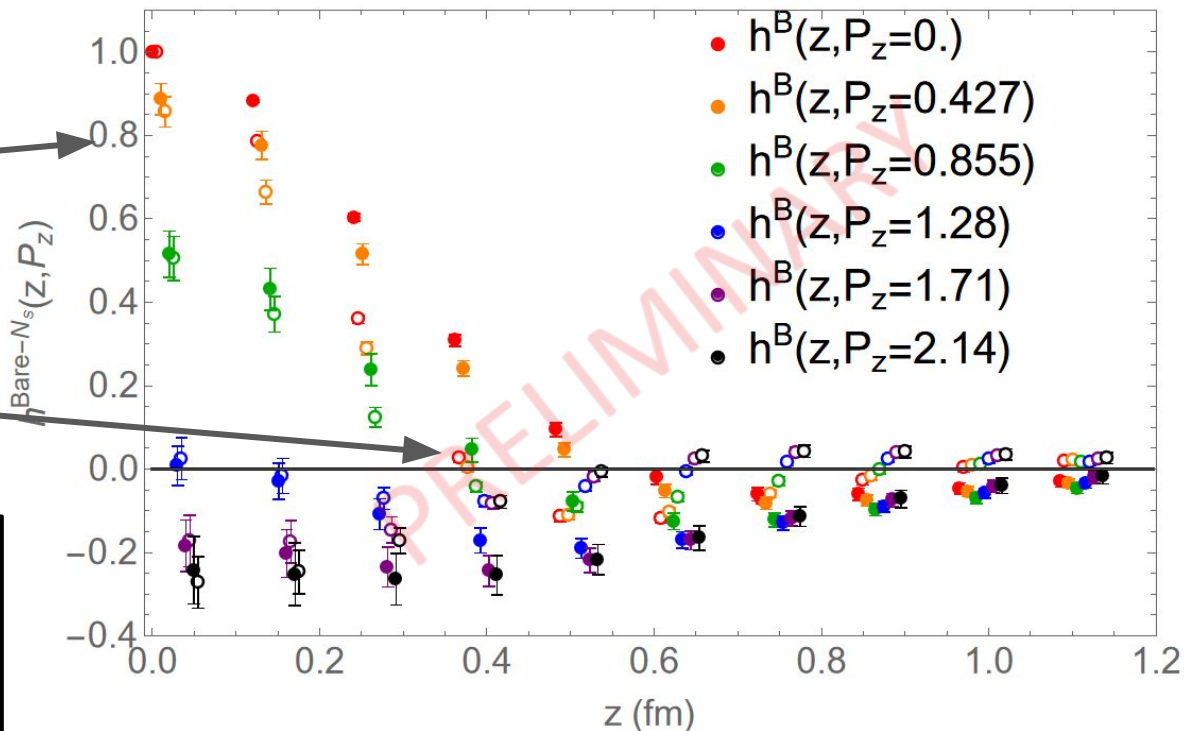
Bare Matrix Elements

- Bare CG (open circles) and gauge invariant (GI) (closed circles) matrix elements:

Agreement with local operator

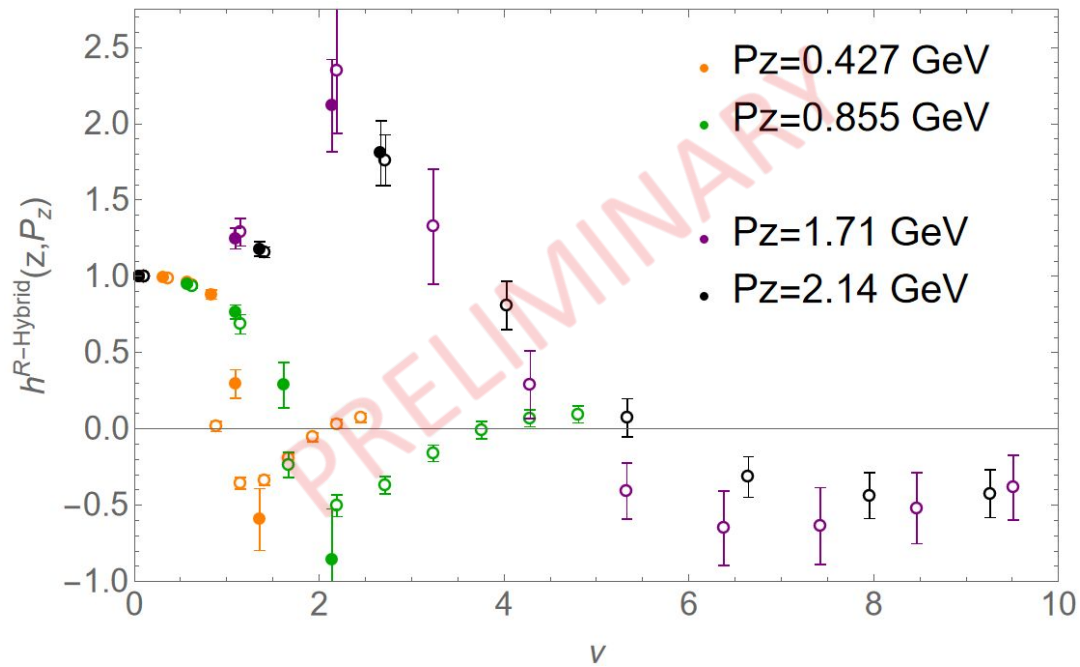
More rapid decay and different zero crossing

Hard to tell if there's signal improvement here, both the important part is hybrid renormalization



Hybrid-Ratio Renormalized Matrix Elements

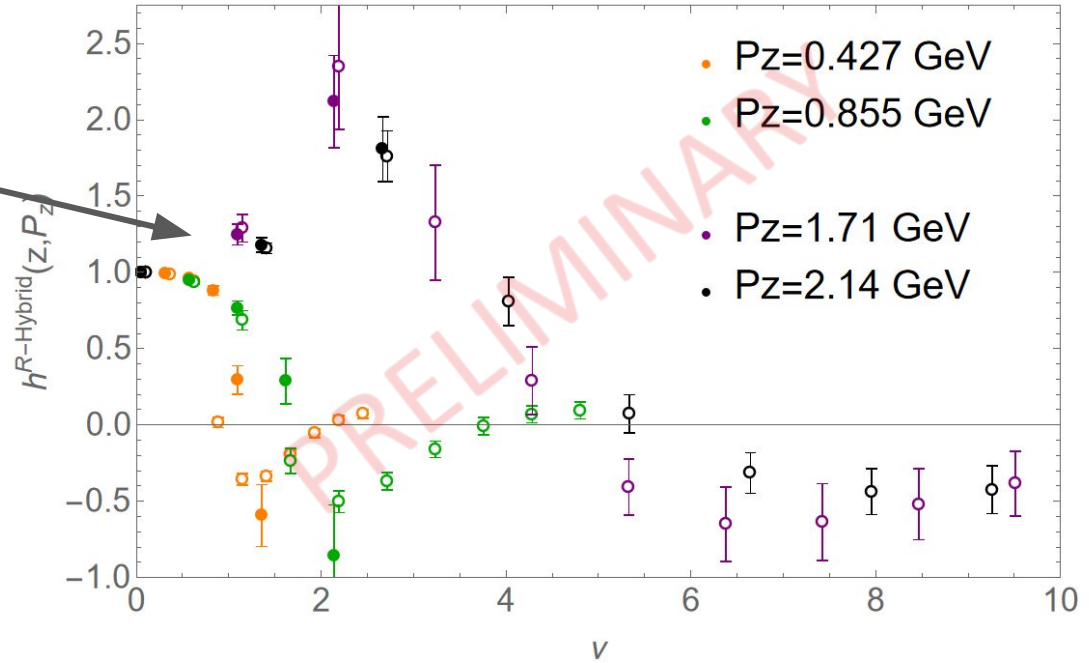
- Hybrid-ratio renormalized CG (open circles) and gauge invariant (GI) (closed circles) matrix elements:



Hybrid-Ratio Renormalized Matrix Elements

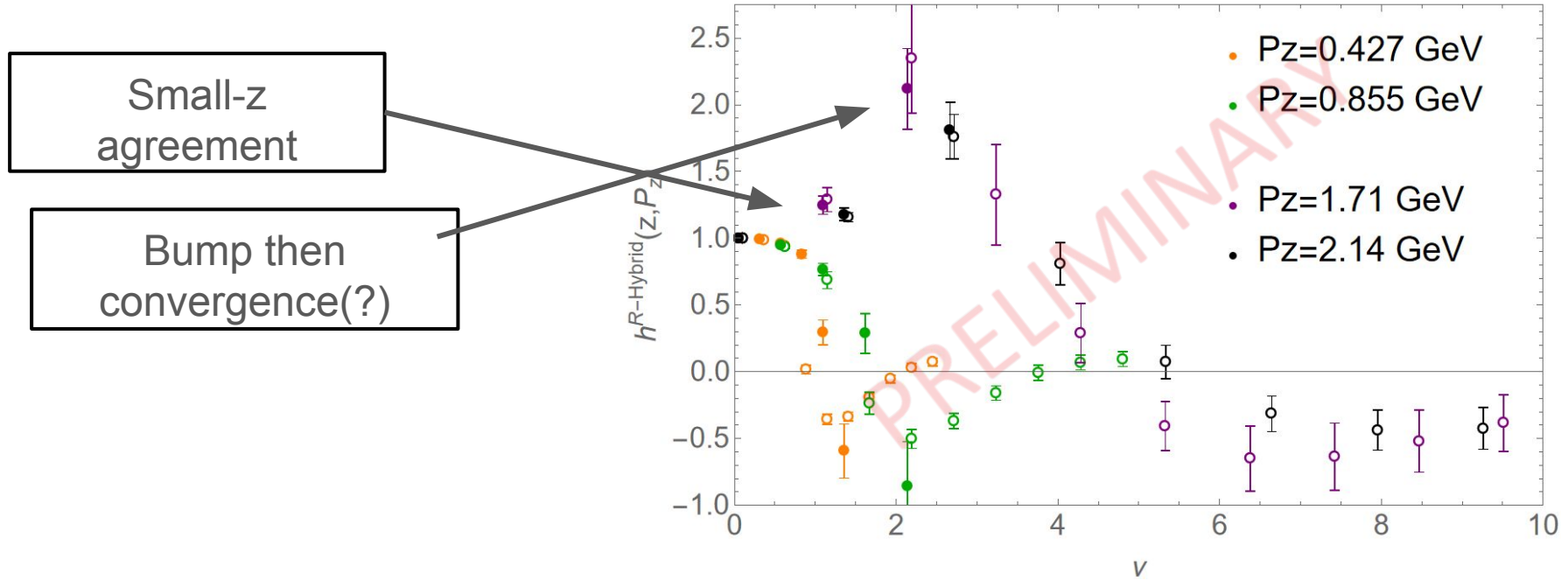
- Hybrid-ratio renormalized CG (open circles) and gauge invariant (GI) (closed circles) matrix elements:

Small-z
agreement



Hybrid-Ratio Renormalized Matrix Elements

- Hybrid-ratio renormalized CG (open circles) and gauge invariant (GI) (closed circles) matrix elements:



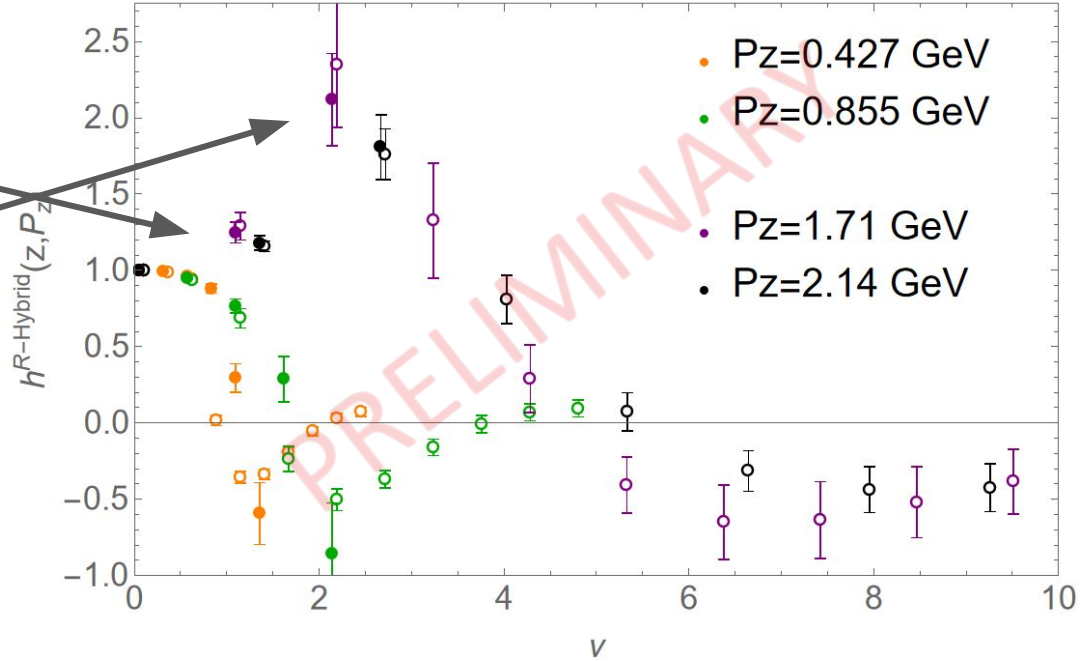
Hybrid-Ratio Renormalized Matrix Elements

- Hybrid-ratio renormalized CG (open circles) and gauge invariant (GI) (closed circles) matrix elements:

Small-z agreement

Bump then convergence(?)

Still a sign change and non-monotonic P_z behavior: Maybe P_z dependent contamination?



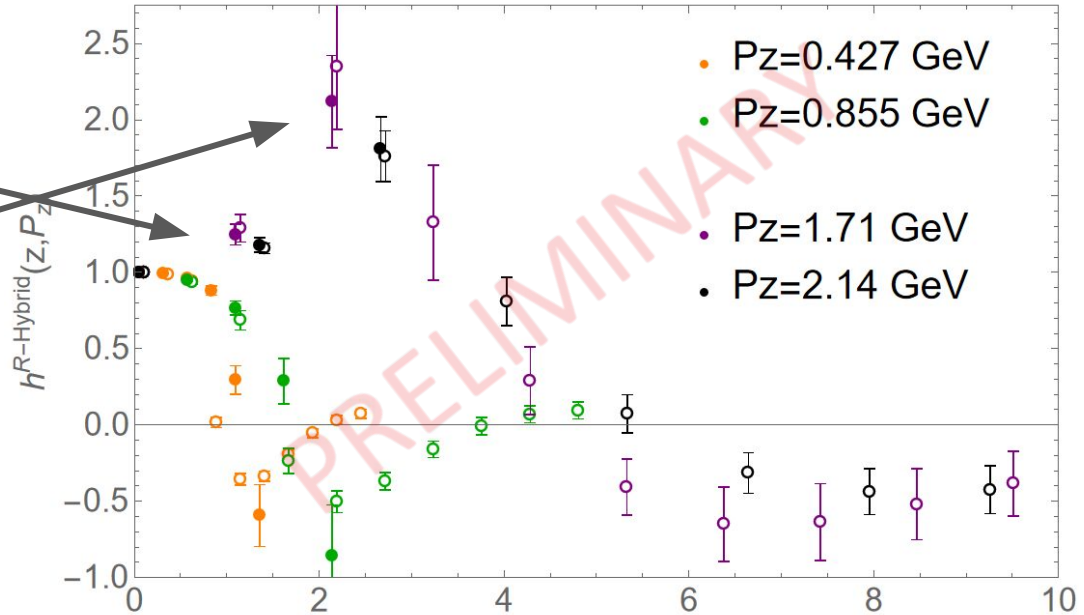
Hybrid-Ratio Renormalized Matrix Elements

- Hybrid-ratio renormalized CG (open circles) and gauge invariant (GI) (closed circles) matrix elements:

Small-z agreement

Bump then convergence(?)

Still a sign change and non-monotonic P_z behavior: Maybe P_z dependent contamination?



Obviously need smearing, hadron, lattice spacing, volume, etc. tests.

Conclusions

- For our lattice setup, we see that $O^{(1)}(z)$ and $O^{(2)}(z)$: perform very poorly in terms of noise and general behavior

Conclusions

- For our lattice setup, we see that $O^{(1)}(z)$ and $O^{(2)}(z)$: perform very poorly in terms of noise and general behavior
- We see that with a guess for the hybrid renormalization of $O^{(3)}(z)$: we can get a somewhat reasonable quasi-PDF

Conclusions

- For our lattice setup, we see that $O^{(1)}(z)$ and $O^{(2)}(z)$: perform very poorly in terms of noise and general behavior
- We see that with a guess for the hybrid renormalization of $O^{(3)}(z)$: we can get a somewhat reasonable quasi-PDF
- This suggests that the Wilson coefficients and hybrid ratio matching kernels should be calculated for $O^{(3)}(z)$:

Conclusions

- For our lattice setup, we see that $O^{(1)}(z)$ and $O^{(2)}(z)$: perform very poorly in terms of noise and general behavior
- We see that with a guess for the hybrid renormalization of $O^{(3)}(z)$: we can get a somewhat reasonable quasi-PDF
- This suggests that the Wilson coefficients and hybrid ratio matching kernels should be calculated for $O^{(3)}(z)$:
- We are also the first to test measuring the gluon operators in the Coulomb gauge and see possible improvement, but more exploration is needed here

Conclusions

- For our lattice setup, we see that $O^{(1)}(z)$ and $O^{(2)}(z)$: perform very poorly in terms of noise and general behavior
- We see that with a guess for the hybrid renormalization of $O^{(3)}(z)$: we can get a somewhat reasonable quasi-PDF
- This suggests that the Wilson coefficients and hybrid ratio matching kernels should be calculated for $O^{(3)}(z)$:
- We are also the first to test measuring the gluon operators in the Coulomb gauge and see possible improvement, but more exploration is needed here
- We need to (and are) considering further ways to improve signal

Bill's Birthday Wishes

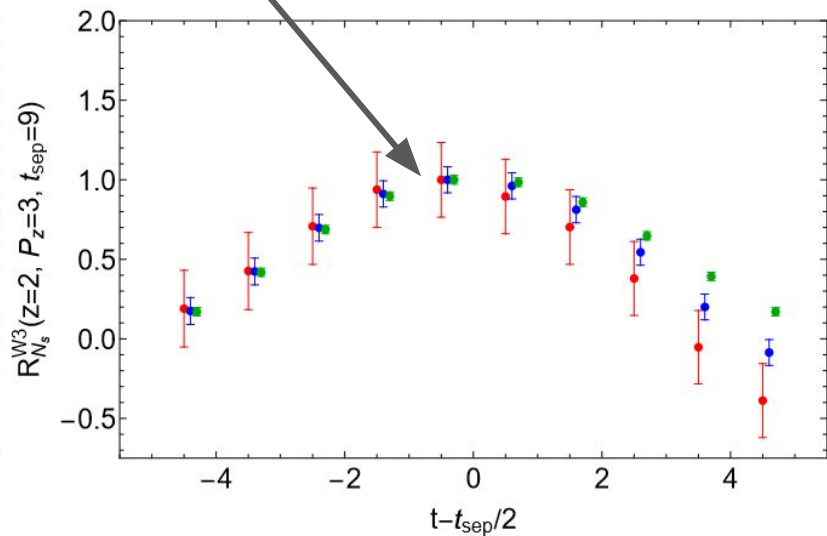
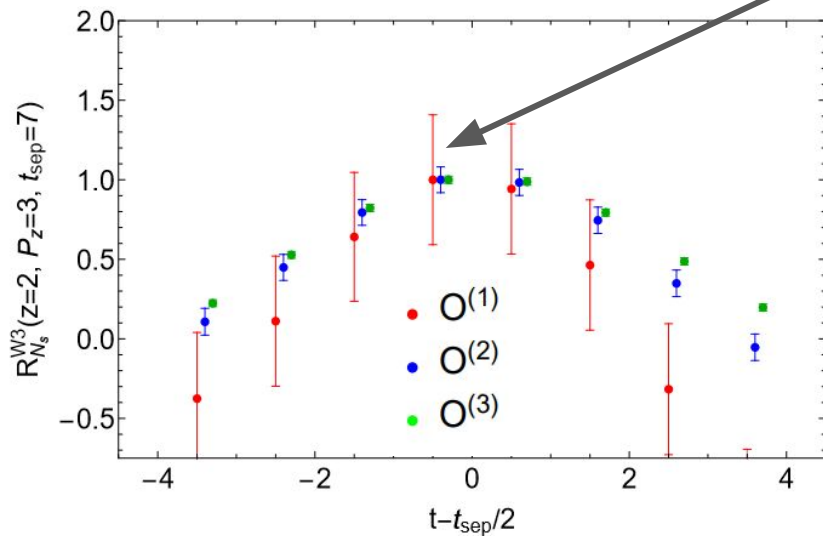
- Hybrid-ratio matching kernels and Wilson coefficients for $O^{(3)}(z)$ (and the other operators not mentioned here)
- Proof (or disprove) that Coulomb gauge fixing is valid for the gluon operators
 - Matching kernels for each operator in this study, if valid
- Any other algorithmic improvements
- A million dollars

Backup

Operator Signal Comparison

- As a first test of which operators are performing better, we can plot the ratio of the 3pt to the 2pt correlators for each operator
- We show the strange nucleon with W3 smearing
- Normalized to such that mean of the center (left) point is 1 so that these can be directly compared

$$R_H(P_z; t_{\text{sep}}, t) = \frac{C_H^{3\text{pt}}(P_z; t_{\text{sep}}, t)}{C_H^{2\text{pt}}(P_z; t_{\text{sep}})}$$

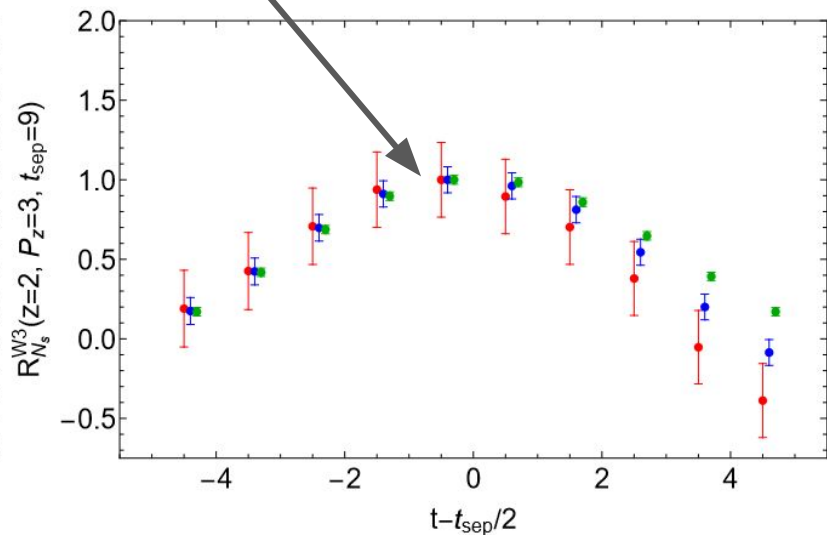
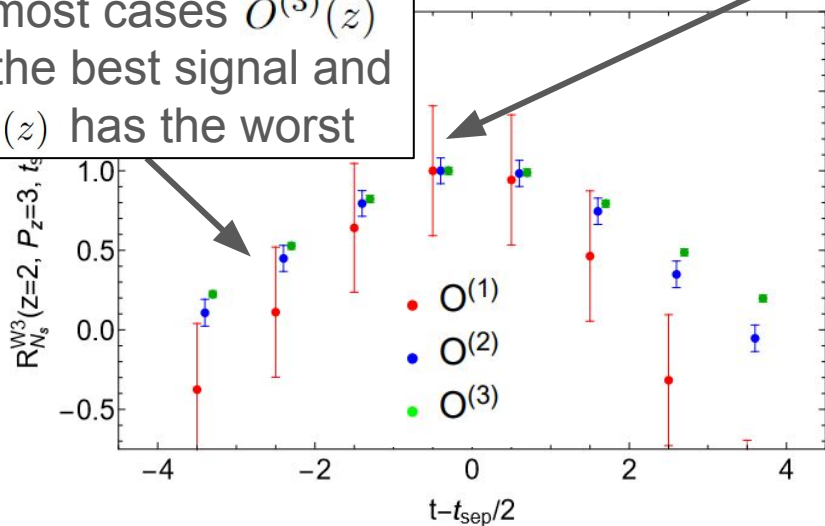


Operator Signal Comparison

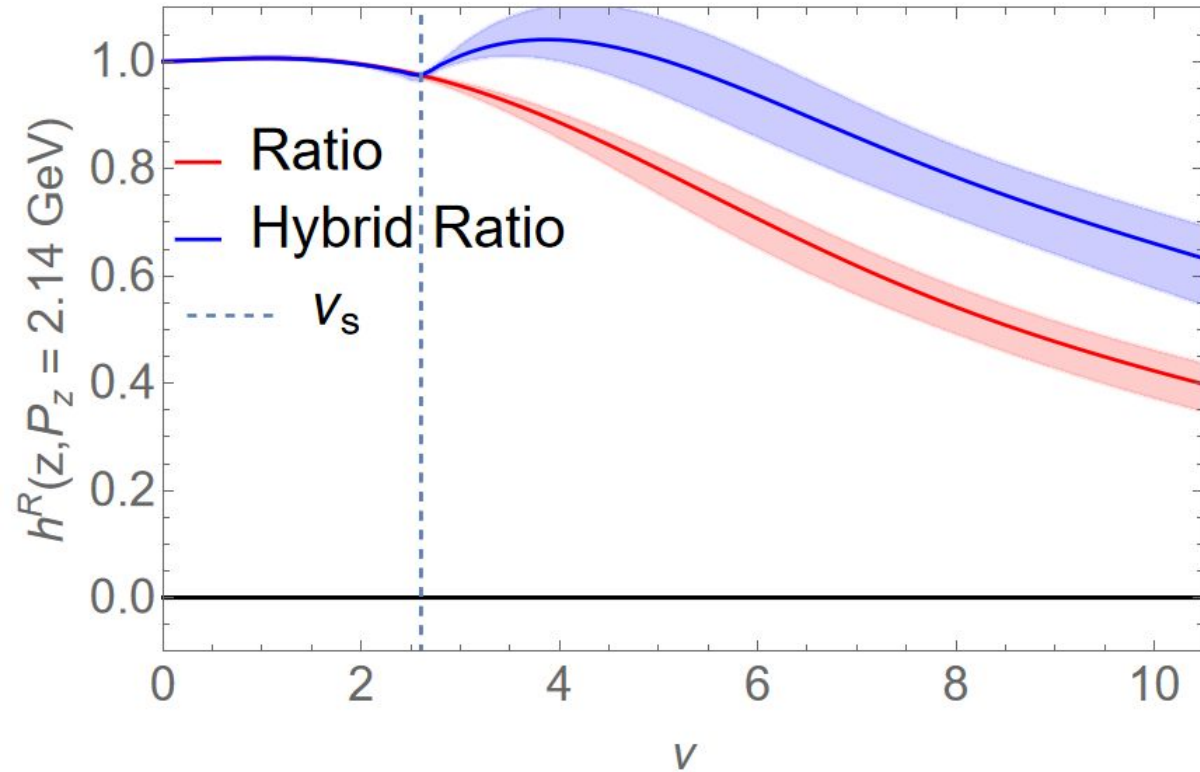
- As a first test of which operators are performing better, we can plot the ratio of the 3pt to the 2pt correlators for each operator
- We show the strange nucleon with W3 smearing
- Normalized to such that mean of the center (left) point is 1 so that these can be directly compared

$$R_H(P_z; t_{\text{sep}}, t) = \frac{C_H^{3\text{pt}}(P_z; t_{\text{sep}}, t)}{C_H^{2\text{pt}}(P_z; t_{\text{sep}})}$$

In most cases $O^{(3)}(z)$ has the best signal and $O^{(1)}(z)$ has the worst



Comparing Pheno. Ratio and Hybrid

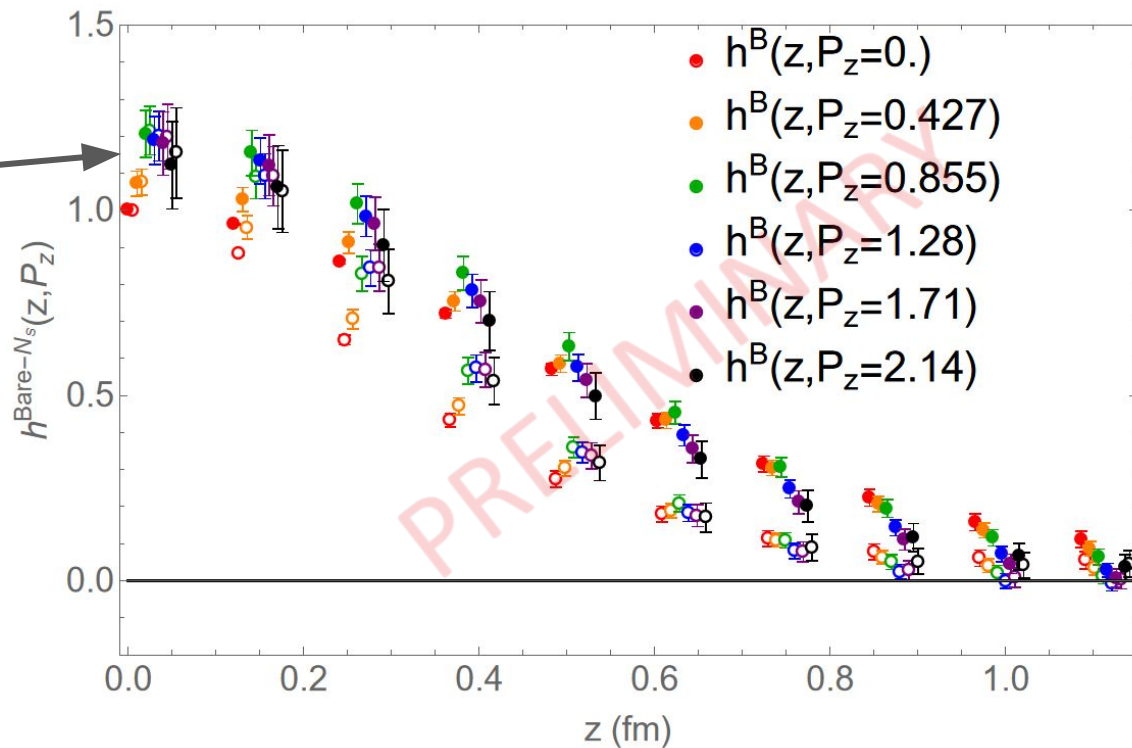


(Also, good agreement with very large z_s)

$O^{(3)}(z)$ Bare Matrix Elements

- Bare CG (open circles) and gauge invariant (GI) (closed circles) matrix elements:

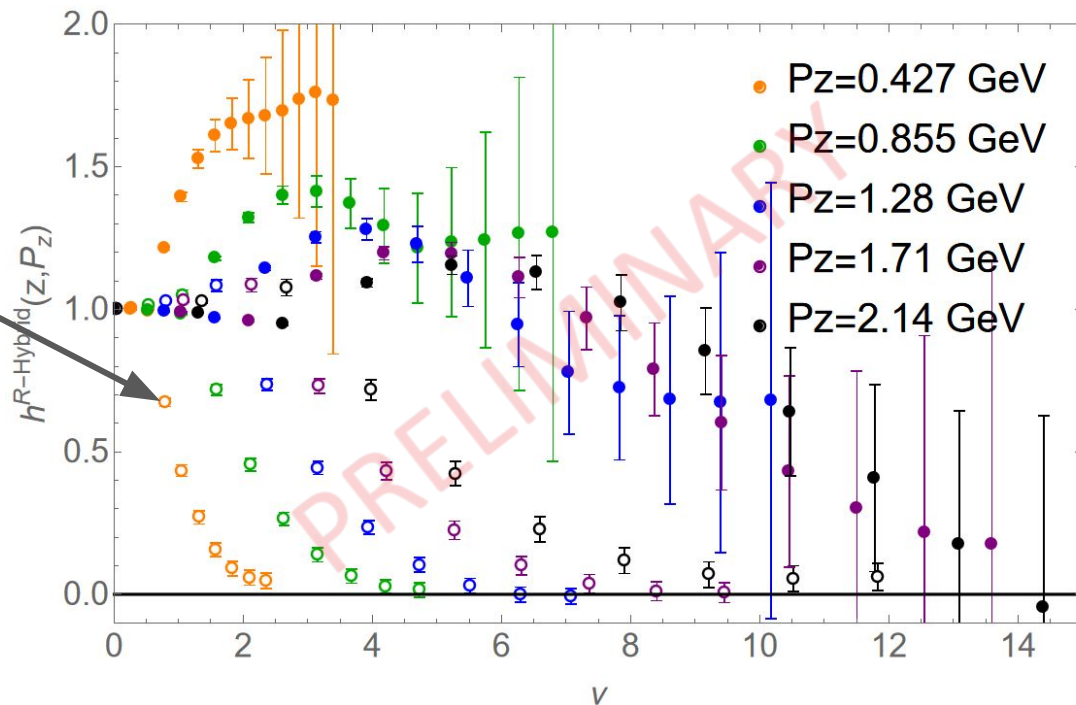
Agreement with
local operator



$O^{(3)}(z)$ Hybrid-Ratio Renormalized Matrix Elements

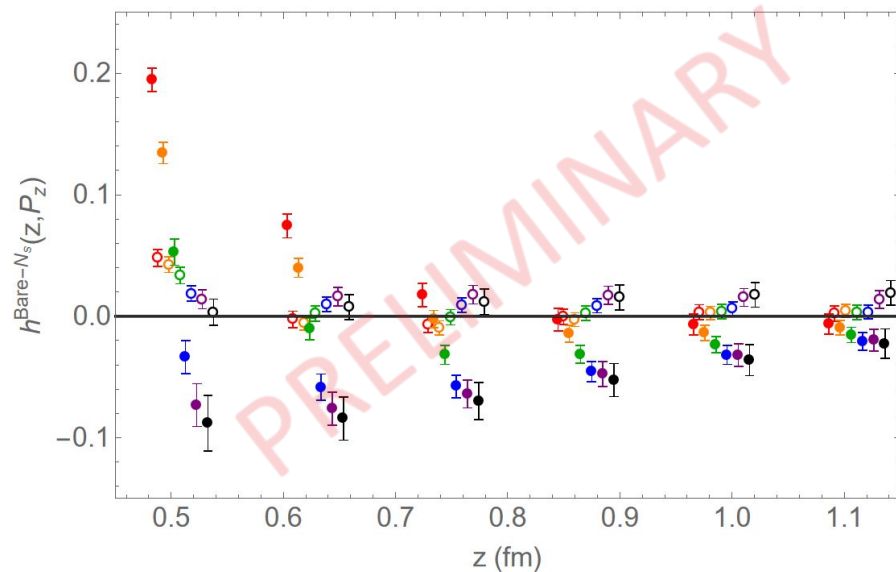
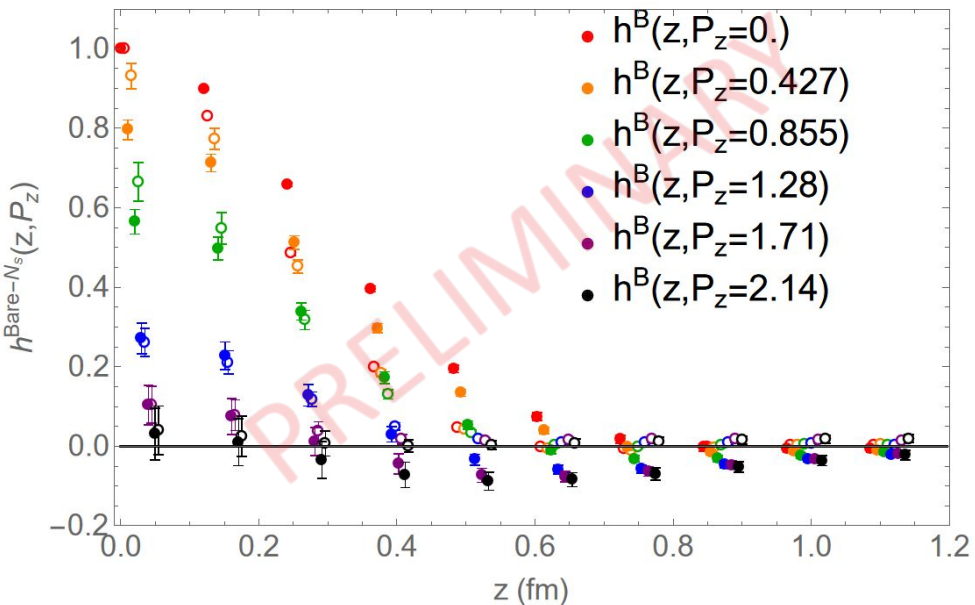
- Hybrid-ratio renormalized CG (open circles) and gauge invariant (GI) (closed circles) matrix elements:

VERY rapid decay?



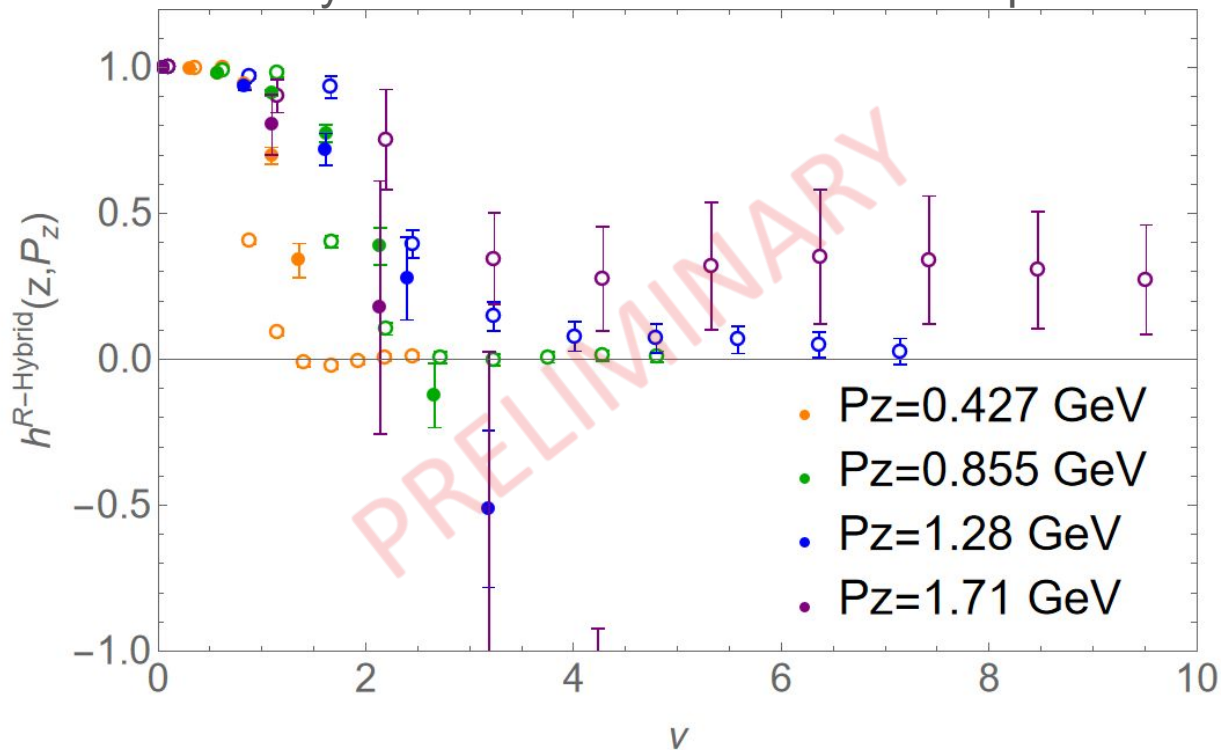
$O(2)$ CG Fixing Results

- Less zero crossings



$O^{(2)}$ CG Fixing Results

Agreement at small- z . Noisy P_z behavior No Pheno. to compare with



Other Concern About $O^{\wedge}(1)$

Lorentz decomposition of the operator:

$$M_{3i;i3} = 2p_3^2 \mathcal{M}_{pp} + 2z_3^2 \mathcal{M}_{zz} + 2z_3 p_3 (\mathcal{M}_{zp} + \mathcal{M}_{pz}) - 2\mathcal{M}_{gg} , \quad (2.8)$$

No information about the relevant matrix element at $P_z = 0$

Balitsky, *et al.*, PLB 808:135621 (2020)